NUMERICAL INVESTIGATION ON HEAT TRANSFER FROM A PHASE CHANGE MATERIAL BASED HEAT SINK WITH AND WITHOUT BAFFLES

A PROJECT REPORT

submitted by

ATHULYA K S

TKM20MEIR04

to

the APJ Abdul Kalam Technological University
in partial fulfilment of the requirements for the award of the Degree

of

Master of Technology

in

Industrial Refrigeration and Cryogenic Engineering

Department of Mechanical Engineering

THANGAL KUNJU MUSALIAR COLLEGE OF ENGINEERING

KOLLAM

JULY 2022

DEPARTMENT OF MECHANICAL ENGINEERING

TKM COLLEGE OF ENGINEERING, KOLLAM

CERTIFICATE

This is to certify that the report entitled '**NUMERICAL INVESTIGATION ON HEAT TRANSFER FROM A PHASE CHANGE MATERIAL BASED HEAT SINK WITH AND WITHOUT BAFFLES**' submitted by '**ATHULYA K S**' to the APJ Abdul Kalam Technological University in partial fulfillment of the requirements for the award of the Degree of Master of Technology in Industrial Refrigeration and Cryogenic Engineering is a bonafide record of the project work carried out by her under my guidance and supervision. This report in any form has not been submitted to any other University or Institute for any purpose.

Internal Supervisor

Dr. LEENA R. 7/7/22

Assistant Professor

Department of Mechanical Engineering

T K M C E, Kollam

PG Coordinator:

Dr. Shafi K A

Professor

Department of Mechanical Engineering

T K M C E, Kollam

Head of the Department:

Dr. Dileep P N

Professor

Department of Mechanical Engineering

T K M C E, Kollam

DECLARATION

I undersigned hereby declare that the project report "Numerical investigation on heat transfer from a phase change material based heat sink with and without baffles", submitted for partial fulfilment of the requirements for the award of degree of Master of Technology of the APJ Abdul Kalam Technological University, Kerala is a bonafide work done by me under supervision of **Dr. Leena R.** This submission represents my ideas in my own words and where ideas or words of others have been included, I have adequately and accurately cited and referenced the original sources. I also declare that I have adhered to ethics of academic honesty and integrity and have not misrepresented or fabricated any data or idea or fact or source in my submission. I understand that any violation of the above will be a cause for disciplinary action by the institute and/or the University and can also evoke penal action from the sources which have thus not been properly cited or from whom proper permission has not been obtained. This report has not been previously formed the basis for the award of any degree, diploma or similar title of any other University.

Athulya K S
University Register No: TKM20MEIR04 of year 2020-2022

Dr. Leena R.
Assistant Professor
Dept. of Mechanical Engineering
T K M C E, Kollam

Head of the Department:

Dr. Dileep P N
Head of the Department
Dept. of Mechanical Engineering
T K M C E, Kollam

July 2022

ACKNOWLEDGEMENT

Any attempt at any level cannot be satisfactorily completed without the support and guidance of learned people. I owe to great many people whose constant support and motivation that has encouraged me to come up with this project.

Firstly, I would like to express my heartfelt thanks to **Dr. Leena R.**, Assistant professor, Department of Mechanical Engineering, TKM College of Engineering for being instrumental in the completion of my project with her guidance. I express my deep sense of gratitude to thank **Dr. Mohammed Sajid N K**., Professor and former Head of Department, and **Dr. Mohammed Sadhikh**, Professor, former PG Co-ordinator, Department of Mechanical Engineering, TKM College of Engineering from bottom of heart for lending me all facilities and support.

I would like to thank **Dr. Dileep P N**, Professor and Head of Department, Department of Mechanical Engineering, TKM College of Engineering for the support to complete this project. I thank **Dr. Shafi K A**, PG co-ordinator, Department of Mechanical Engineering, TKM College of Engineering for giving their constant support for doing this project.

ATHULYA K S

ABSTRACT

For cooling portable electronic devices, effective thermal management (TM) depending on phase change material (PCM) is used. To absorb the thermal energy that all such devices release, PCM is used in the heat sink. The aim of this study is to determine how to increase the charging period of PCM. This work reports the results of detailed numerical studies carried out to improve the performance of a PCM-based heat sink in the charging cycle using baffles. Baffles are horizontal plate-fin structures made of aluminium. Two numerical studies were carried out. The first one is a comparative studyon heat transfer from PCM-based heat sinks with and without baffles. The PCM used is n-eicosane. The second one is a comparative study of two PCMs, rubitherm and n- eicosane. And validation of experimental data is done. From the numerical study a heat sink with baffles filled with a 0.9 volumetric fractionof n-eicosane shows the best performance. Rubitherm filled in the heat sink without baffles shows the best heat transfer. The investigation of PCM-based heat sinks with and without baffles revealed that more than 51% of the temperature differential was caused by baffles.

Keywords: Baffles, phase change material, Rubitherm, N-eicosane, Charging time.

CONTENTS

Title	Page number
AKNOWLEDGEMENT	i
ABSTRACT	ii
LIST OF TABLES	vii
LIST OF FIGURES	viii
ABBREVIATIONS	xi
NOTATIONS	xii
Chapter 1 Introduction	1
1.1 General background	1
1.1.1 Thermal management	2
(i) Active cooling methods	4
(ii) Passive cooling methods	4
1.2 Problem formulation	5
1.3 Objectives	6
1.4 Methodology	6
1.5 Organization of thesis	7
Chapter 2 Literature review	8
Chapter 3 Heat sink	12
3.1 Active heat sinks & Passive heat sinks	13
Chapter 4 Phase-change material-based heat sink	15
4.1 Sensible heat storage & latent heat storage	16
4.2 Classification of PCM	18
4.3 Properties of PCM	19
4.4 Advantages of phase change energy storage	21
4.5 Economical & environmental benefits	21
4.6 Thermal conductivity enhancers	22
Chapter 5 CFD simulation	23
5.1 Introduction to CFD	23
5.2 CFD applications	23
5.3 Numerical methods used in CFD	23
5.3.1 Finite Difference Method (FDM)	24

5.3.2 Finite Element Method (FEM) 24
5.3.3 Finite Volume Method (FVM) 24
5.4 Advantages of CFD over experiment methods 25
5.5 Working of a CFD code 25
5.5.1 Pre-processor 26
5.5.2 Solver 26
5.5.3 Post-processor 27
5.6 Problem solving with CFD 27
5.7 Computational fluid dynamics simulation 27
5.8 Phases of modelling and simulation 29
5.9 CFD calculation 31
Chapter 6 Numerical study on heat transfer 33
6.1 Introduction 33
6.2 Validation of experimental data 33
6.2.1 Computational domain 34
6.2.2 Mesh domain of pin-fin heat sink 35
6.2.3 Initial and boundary Conditions 36
6.3 Numerical study of heat sink with baffles and without baffles 39
6.3.1 Computational domain of heat sink without baffles 40
6.3.2 Mesh domain of heat sink Without baffles 41
6.3.3 Computational domain of heat sink with baffles 43
6.3.4 Mesh domain of heat sink with baffles 44
6.3.5 Initial and boundary conditions 45
6.4 Conduct a comparative study between N-eicosane & Rubitherm PCMs 46
Chapter 7 Results and discussion 47
7.1 Numerical validation of experimental data 47
7.1.1 Effect of heat sink Configurations 47
7.1.2 Effect of PCM amount 49
7.1.3 Effect of heat flux 50
7.1.4 Latent heat phase Comparison 51

7.2 Numerical study of heat sink with and without baffles 53
7.2.1 Variation of charging period in PCM based heat sink without baffles 53
7.2.2 Variation of liquid Fraction of PCM in without baffles 54
7.2.3 Variation of charging Period in PCM based Heat sink with baffles 54
7.2.4 Variation of liquid Fraction of PCM in with Baffles. 55
7.3.5 Temperature comparison between with and without baffles 56
7.2.6 Liquid-fraction Comparison between with & without baffles 57
7.3 Comparative study between N-eicosane & Rubitherm PCMs 58
7.3.1 Variation of charging Period in PCM Based Heat sink without (Rubitherm) 58
7.3.2 Variation of liquid Fraction of Rubitherm 59
7.3.3 PCM-based heat sink Without baffles (temperature) 59
7.3.4 PCM-based heat sink Without baffles (Liquid-fraction) 61
7.3.5 Variation of charging Period in PCM Based Heat sink with baffles (Rubitherm) 62
7.3.6 Variation of the liquid Fraction of Rubitherm (with baffles) 62
7.3.7 PCM-based heat sink with baffles (temperature) 63
7.3.8 PCM-based heat sink with baffles (Liquid-fraction) 64

Chapter 8 Conclusion 65
References 66

LIST OF TABLES

Title	Page number
Table 4.3.1 Properties of PCM.	20
Table 6.2.3.2 Properties of n-eicosane.	38
Table 6.3.3.3 Properties of Aluminium.	44
Table 6.4.4 Properties of Rubitherm.	46
Table 7.1.3.5 Enhancement in time to reach 40˚C, 3mm thickness pin fin heat sink.	51
Table 7.2.4.6 Comparison of temperature.	56
Table 7.2.5.7 Comparison of the liquid fraction.	57
Table7.3.3.8 Temperature comparison between rubitherm and n-eicosane (without baffles).	60
Table7.3.4.9 Liquid fraction comparison between rubitherm & n-eicosane (without baffles).	61
Table 7.3.7.10 Temperature comparison between rubitherm and n-eicosane (with baffles).	63
Table 7.3.8.11 Liquid fraction comparison between rubitherm and n-eicosane (with baffles).	64

LIST OF FIGURES

Title	Page number
Fig.1.1.1.1 Tree of methods of removing heat from the hot source surface.	3
Fig.1.4.2 Methodology flow chart	7
Fig.3.1.3 Passive heat sink.	13
Fig.3.1.4 Active heat sink.	14
Fig.4.5 Working of PCM.	15
Fig.4.1.6 Sensible heat & latent Heat.	17
Fig.4.1.7 Temperature control during phase change Energy storage.	17
Fig.4.2.8 Classification of PCM.	18
Fig.4.6.9 Rectangular heat sink.	22
Fig.4.6.10 Pin fin heat sink.	22
Fig.5.8.11 Phases of modelling and simulation	29
Fig.6.2.12 Dimensions of 4 mm thick pin-fin heat sink.	34
Fig.6.2.1.13 Geometry of 4 mm thick pin fin PCM-based heat sink.	34
Fig.6.2.2.14 Meshing of heat sink.	35
Fig.6.2.2.15 Grid independence study.	36
Fig.6.2.3.16 Positions of thermocouples on a heat sink.	37
Fig.6.3.17 dimensions of heat sink without baffles.	39
Fig.6.3.18 a & b computational domain of heat sink Without baffles	41
Fig.6.3.2.19 Meshing of heat sink without baffles.	42
Fig.6.3.2.20 Grid independence study of heat sink Without baffles.	42
Fig 6.3.3.21a & b Computational domain of heat sink Without baffles	43
Fig.6.3.4.22 Meshing of the heat sink with baffles.	44
Fig.6.3.4.23 Grid independence study of the heat sink With baffles	45

Fig. 7.1.1.24a Effect of fin thickness for ψ = 0.3 at 1.6 kW/m^2 47
Fig.7.1.1.24b Effect of fin thickness for ψ = 6 at 1.6 kW/m^2 48
Fig.7.1.1.24c Effect of fin thickness for ψ = 9 at 1.6 kW/m^2 48
Fig.7.1.2.25 Time-temperature distribution for no fin heat sink at different ψ. 49
Fig.7.1.3.26 Phase change variations at different input Heat fluxes for 3 mm pin-fin heat sink. 50
Fig.7.1.4.27 Latent heating phase completion durations For different configuration heat sinks. 51
Fig.7.2.1.28 temperature-time graph (heat sink without Baffles) 53
Fig.7.2.2.29 Liquid fraction – time graph (heat sink Without baffles) 54
Fig.7.2.3.30 temperature-time graph (heat sink with Baffles) 55
Fig.7.2.4.31 liquid fraction-time graph (heat sink with Baffles) 55
Fig.7.2.4.32 temperature comparison. 56
Fig.7.2.5.33 Liquid fraction comparison. 57
Fig. 7.3.1.34 Temperature-time graph of Rubitherm (Without baffles). 58
Fig.7.3.2.35 Liquid fraction of Rubitherm (without baffles). 59
Fig.7.3.3.36 comparison between rubitherm temperature & n-eicosane temperature (without baffles) 60
Fig.7.3.4.37 comparison of the liquid fraction of rubitherm and n-eicosane (without baffles). 61
Fig.7.3.5.38 Temperature-time graph of Rubitherm (With baffles). 62
Fig.7.3.6.39 Liquid fraction of rubitherm (with baffles). 62

Fig.7.3.7.40 comparison between rubitherm temperature & n-eicosane temperature (with baffles). 63

Fig.7.3.8.41 Comparison of the liquid fraction of rubitherm and n-eicosane (with baffles). 64

ABBREVIATIONS

CFD Computational Fluid Dynamics

HSU heat storage unit

LHSS latent heat storage system

PCM Phase change material

PRESTO Pressure Staggering Option

SIMPLE Semi-Implicit Method for Pressure Linked Equations

TCE Thermal conductivity enhancers

TM Thermal management

SIMPLE Semi-Implicit Method for Pressure Linked Equations

NOTATIONS

C_p	Specific heat, kJ/kg˚C
h_l	Specific latent heat, kJ/kg
m	Mass, kg
$Q_{sensible}$	Sensible heat, kJ
Q_{latent}	Latent heat, kJ
q	Heat flux, kJ
ΔT	Temperature difference, ˚C

Greek symbols

Ψ	volumetric fraction of PCM

CHAPTER 1

INTRODUCTION

1.1 GENERAL BACKGROUND

Thermal management has become more important in industry due to the advancement of technology. The primary objective of thermal management is to remove heat from the thermal devices to ensure that they operate properly and to avoid triggering temperature-activated failure mechanisms. This is generally accomplished by conducting the heat away from the thermal bodies and into a gas or liquid coolant. However, the power dissipation of electrical devices like microprocessors has increased dramatically in recent years. This change has provided thermal engineers with the challenges of managing the increasing thermal budget in order to maintain the device at a safe operating temperature because the conventional cooling solutions reach their limits. With the increase in thermal power generation, new cooling solutions continue to be investigated.

Nowadays electronic devices play a vital role in different operations in our life. The size of electronic devices is getting abbreviated with every passing day, at the same time their computing power is continuously on the rise. However, an inevitable by-product, heat is produced continuously from these electronic devices. Hence it is required to cool the devices and maintain their temperature and requires better management to remain within the safety limits. The failure rate increases exponentially with the rising temperature which means that a smaller increase in operating temperature may lead to failure or performance of the devices. So, there is an immense need for an efficient cooling system to dissipate this heat for a comfortable operating temperature. Therefore, good thermal management is two cooling techniques are used, active and passive techniques. According to the applications passive cooling techniques are mostly used. Devices that use passive cooling are more portable and don't need additional power to cool. One of the frequently employed passive-type heat exchangers is a heat sink. The sensible heat capacity of the fluid inside a heat sink is the primary factor affecting the heat sink's ability to dissipate heat.

To make use of the benefits of both sensible and latent heat in a small volume, a phase change material (PCM) is used as the working medium in a heat sink. The PCM for a given application is chosen so that its melting temperature is lower than the device's maximum working temperature. The majority of PCMs possess the qualities of high latent heat of fusion, high specific heat, high storage density, good chemical stability, nonflammability, and good cycling stability; however, PCMs have low thermal conductivity (typically 0.5 W/m.K.), necessitating the use of techniques to improve heat transfer. The high storage density of the PCM aids in regulating the rise in temperature of electronics and keeps it at a relatively steady level for a longer period.

To enhance the thermal conductivity property of PCM, thermal conductivity enhancers (TCE) are used. They are in the form of fins, metal foams, and nanoparticles that are almost invariably used in combination with PCM to increase the effective thermal conductivity of the PCM.

1.1.1 Thermal Management

Due to the high heat fluxes that electronic devices are exposed to, thermal management of these devices is becoming increasingly difficult. Increased power consumption and heat generation inside the system are directly related to the demand for increasing miniaturization and continual performance improvements. Thermal management is a necessity in all electronics goods since excessive heat generation harms a negative impact on user health as well as the dependability and performance of the product. The capacity to regulate a system's temperature and noise level using technology based on thermodynamics and heat transport is known as thermal management. The need for creative thermal management solutions has grown as a result of advancements in the electronics sector. By reducing the high heat flux generated by electronic devices, these technologies can enhance system performance and reliability.

Thermal management of electronic devices includes two types of heat removal methods, namely, direct and indirect heat removal. Direct heat removal techniques include heat sink, forced convection and thermoelectric refrigeration.

Indirect heat removal includes heat pipe, boiling, micro channel cooling, jet impingement cooling, spray cooling, refrigeration etc.

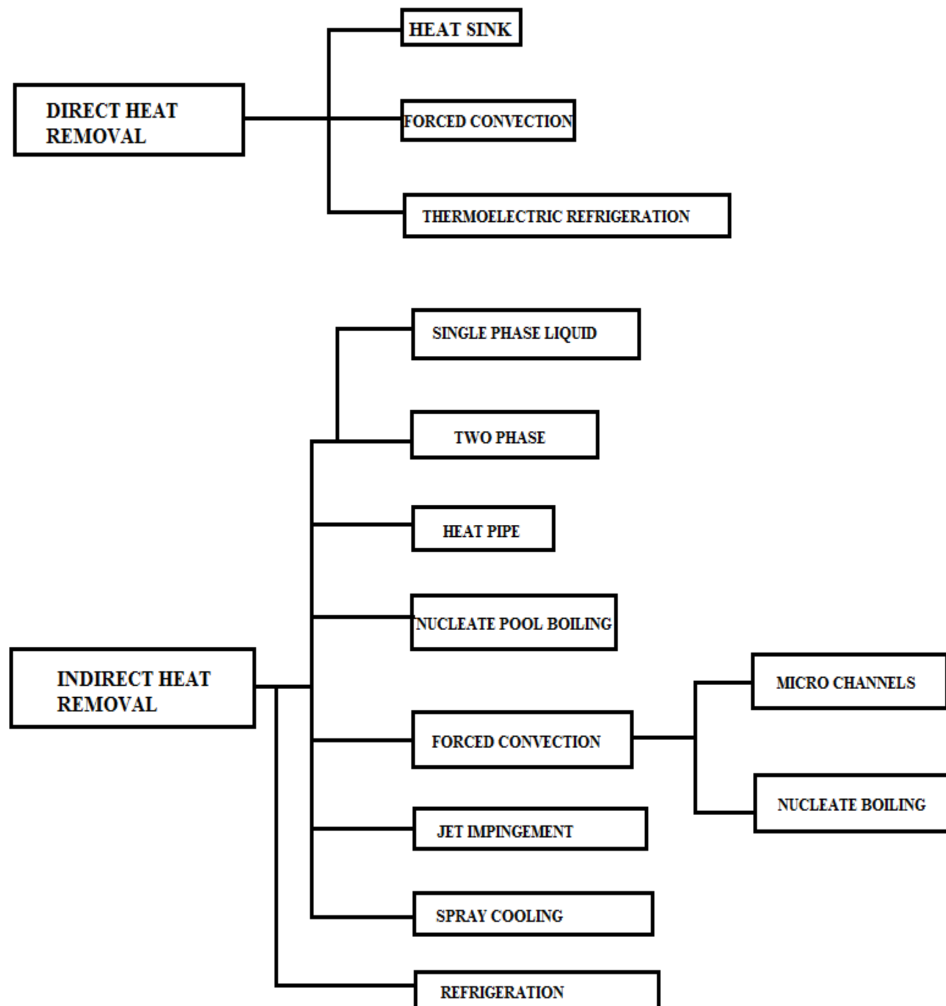

Fig.1.1.1.1 Tree of methods of removing heat from the hot source surface

Direct Heat Removal means heat is directly transferred from source to the ambient. Indirect Heat Removal uses a working fluid to transport heat from the hot source to the heat sink. The term ambient heat sink is defined to mean the final heat rejection device that rejects heat to the ambient, via air or water-cooling. Use of Indirect heat removal establishes the need for a second heat sink located at the hot source. This will be called the ‘‘hot source heat sink’’.

Electrical resistance is the reason for the hard-working computer's temperature increase. A charge imbalance causes electrons to flow through a substance with electrical resistance. These traveling electrons collide with the material's (often crystalline) structure as they go through it, causing friction. Due to the high level of friction, cooling techniques are frequently needed. Fundamentally, there are two types of electronic cooling methods: passive cooling and active cooling.

(i) Active Cooling Methods

The use of cooling fans, correct component spacing, and liquid condensation with heat pipes are examples of active cooling techniques. For designs with high power outputs or microprocessors, active approaches are frequently used. Although they need a power source to function, they are typically more effective at reducing heat through conduction and convection techniques.

Add Space Components and a Cooling Fan. Properly: The addition of a cooling fan significantly lowers temperatures. The ventilation outlet receives warm air that is moved there by the cooling fan. When utilizing a cooling fan, it's crucial to plan the ventilation path. This entails figuring out the air input and outflow and predicting the airflow's direction.

Use Heat Pipes: To transmit heat away from high-temperature components, heat pipes-which are cylindrical copper pipes-are employed. To remove heat through a condenser, heat pipes occasionally have liquids inside of them, such as water. Miniature heat pipes, which conduct heat more effectively and are small enough to be integrated into a PCB, are one recent breakthrough.

(ii) Passive Cooling Methods

Passive cooling methods include the use of heatsinks and thermal vias. These methods don't need a power supply, but they have a limited capacity for heat dissipation. They are appropriate for designs that don't generate a lot of heat. Using a temperature data recorder, which lacks any high-current components, is an illustration of a passive cooling strategy.

Employ a heatsink: Components like power transistors and microprocessors frequently require heatsinks. They have surfaces that resemble fins and structures that resemble baffles, which increase heat transfer to the air. To increase the effectiveness of heat conduction, the heat transfer compound is frequently put between the component and the heatsink. Due to their high latent heat storage capacity, phase change materials (PCMs) are presently the subject of extensive study for effective TM modules to store thermal energy by utilizing a latent heat storage system (LHSS). In an LHSS, heat is captured during high transient and continuous power loads within the PCM and later released to the environment while keeping vital components at a consistent and secure temperature. High latent heat of fusion, high specific heat, congruent melting, and non-corrosiveness are characteristics of PCMs (particularly organic PCMs) with very low thermal conductivity. Different materials with high thermal conductivity, known as thermal conductivity enhancers (TCEs), are employed to overcome the difficulty of PCMs' poor thermal conductivity. It is found that different TCEs e.g., extruded fins, nano-particles, baffles, and metal matrices are embedded in PCM-based LHSS.

1.2 PROBLEM FORMULATION

Nowadays size of the electronic gadgets reducing based on developing criteria for effective working. In the reduction of size in an electronic device where a large amount of heat load is generated that not only leads to malfunctioning but also device failure. In this contest, thermal management is needed, and modern cooling features are to be selected.

The modern cooling techniques are explained in [1.1]. from cooling techniques, passive cooling techniques are more adaptive in electronic devices. Passive cooling devices are more compact. It does not require external energy for cooling. A heat sink is one of the commonly used passive-type heat exchangers. The dissipation capacity of the heat sink is mainly depending on the sensible heat of fluid that flows inside the heat sink. Here we can use a phase change material as the working fluid that is inside the heat sink, which has the advantages of both sensible and latent within the small volume. PCM helps to maintain a constant temperature for a longer period. But the PCM has a very low thermal conductivity. To increase the thermal conductivity, some structures are introduced. That

structures are called thermal conductivity enhancers. Fins, baffles, metal foams, and also nanoparticles are used.

1.3 OBJECTIVES

The main objective is the numerical study (using ANSYS Fluent) on heat transfer from a PCM-based heat sink.

The specific objectives are;

1. To validate the numerical model with the experimental values of literature.
2. To conduct the parametric study (thickness of fin, and heat flux) with baffles and without baffles.
3. To conduct a comparative study between n-eicosane and rubitherm PCMand determine which is more efficient.

1.4 METHODOLOGY

Objective 1: Validate the numerical model with experimental data from Arshad and Ali, et al. (2018).

- Validating the parameters which affect the heat sink effectiveness.
- Optimizing the parameters such as PCM volume, the thickness of fin, and heat flux.

Objective 2: Conduct a numerical study with baffles and without baffles.

- Selection of suitable dimensions.
- Setting up boundary conditions.
- Numerical simulations of with and without baffles are carried out using n-eicosane.

Objective 3: Conduct a comparative study between n-eicosane and Rubitherm PCMs.

- Characteristic study of n-eicosane and Rubitherm.
- Selection of suitable PCM according to the temperature range.
- Numerical simulation using selected PCMs with and without baffles.

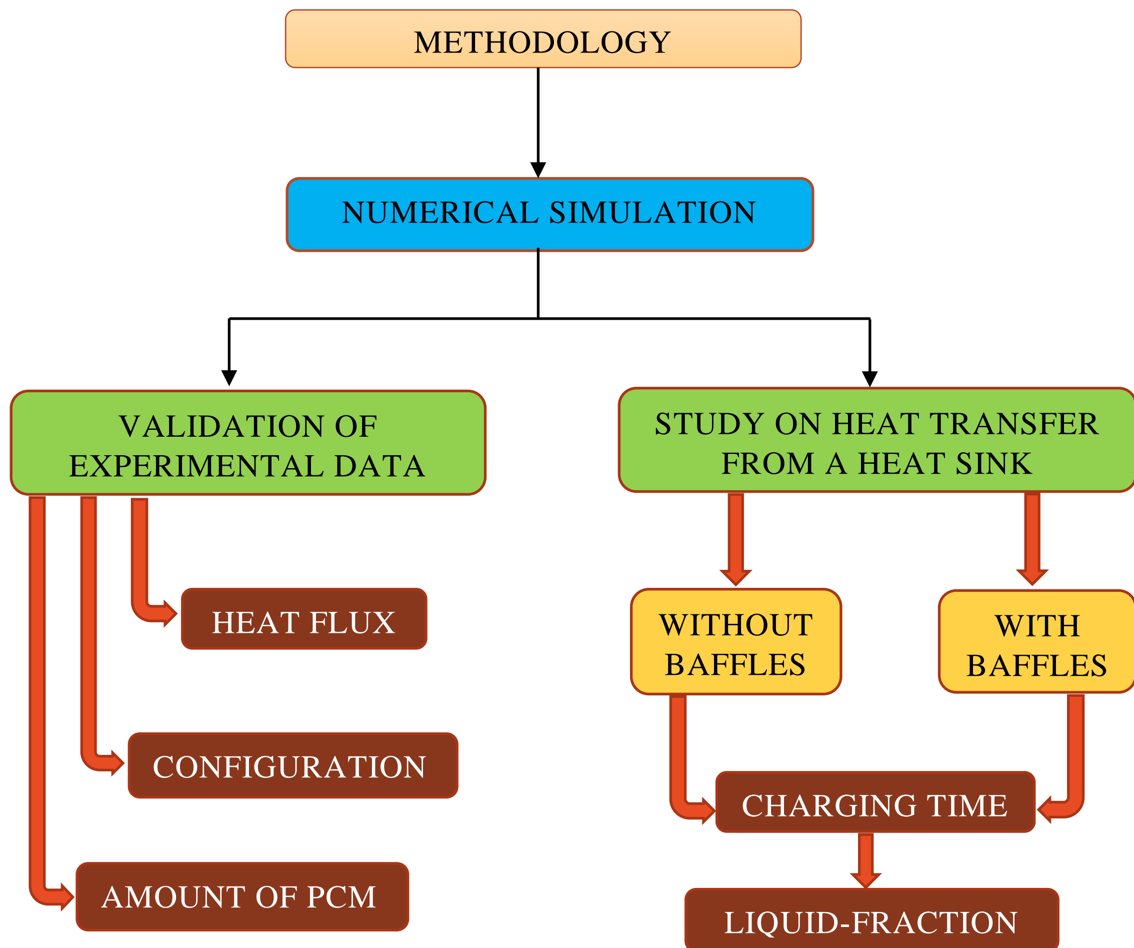

Fig.1.4.2 Methodology flow chart

1.5 ORGANIZATION OF THESIS

The thesis is presented in seven chapters:

Chapter 2 gives review of literature of the studies related to the present investigation.

Chapter 3 discusses about the importance of sinks sink in an electronic device and their types.

Chapter 4 explains about physis of phase change material and the phase change material-based heat sinks.

Chapter 5 numerical investigation of PCM-based heat sink.

Chapter 6 explains the results of each objective.

Chapter 7 summarizes the results of the numerical investigation and conclusions drawn from the results.

CHAPTER 2

LITERATURE REVIEW

Swanson and Birur (2003), outlined different heat control solutions for robotic NASA missions about ten years ago. Schmidt (2004) described the difficulties encountered with managing the thermal needs of computer hardware for a small channel liquid-cooled heat sink.

Tan and co-authors, (2004&2010) used plate-fin PCM-based heat sinks to conduct an extensive and in-depth experimental evaluation of TM in portable mobile devices. Using a heat storage unit (HSU) implanted inside the mobile devices, the impacts of various power levels, fin counts, and orientations were investigated for steady and unsteady operation modes. It was determined that the HSU exposed to a higher power level increased the melting rate and decreased the device's base temperature.

Fan and Khodadadi (2008) concluded that for better performance and increased reliability of the device, the design of the PCM based heat sink should be such that the entire PCM melting should be completed before the chip temperature reaches a critical value.

Saha and co-authors (2008&2010) suggested the ideal arrangement of fins for a heat sink filled with PCM. They employed aluminum as TCE and found that a volume percentage of 8% of TCE was superior for thermal regulation. According to the characteristic length of various enclosures and the appropriate characteristic length for each configuration of plate-fin enclosures, the authors of another study showed several correlations of the dimensionless Nusselt number, Reynolds number, Stefan number, and Fourier number. The parametric effects of plate-fin heat sink filled with PCM were examined in a recent computational and experimental study. (Paraffin wax RT-80). In contrast to fin thickness, it was discovered that increasing the heat sink's number of fins and fin height had a positive impact on the heat sink's performance.

Kandasamy et al. discovered in 2008 that thermal performance and melting rate increase at higher power levels until full melting of the PCM, paraffin wax. Under cyclic steady conditions, the application of a novel PCM package for thermal management of portable electronic devices was investigated experimentally for the effects of various parameters such as power input, package orientation, and various melting/freezing times. A two-dimensional numerical study was also conducted, and the experimental results were compared. The results show that increasing the power input increases the melting rate, while the package's orientation to gravity does not affect the thermal performance of the PCM package. For the design of a passive thermal control system, the thermal resistance of the device and the power level applied to the PCM package is critical. When compared to numerical results, the PCM-based design is an excellent candidate for transient electronic cooling applications.

A pair of ANN-GA approaches were used by Baby and Balaji (2012&2013) to conduct an experimental investigation on the thermal performance of pin-fin heat sinks with volume fractions of 4 percent, 9 percent, and 15 percent TCE. A heat sink's operating time improvement ratio compared to a sink without fins and a PCM was calculated. A heat sink filled with PCM performed significantly better thermally when pin-fins made up 9% of the volume.

To ascertain the impact of heat sink designs on the efficiency of PCM-based heat sinks for cooling electronic devices, Mahmoud et al., (2013), carried out experimental research. They took into consideration a heat sink without any TCE, a heat sink with parallel fins, a heat sink with cross fins, and a honeycomb structure put into a single cavity when they conducted their investigation. They used paraffin wax as the phase change substance in each of the aforementioned instances. According to the experimental findings, a heat sink with TCE had lower temperatures at the end of the charging cycle than a heat sink without TCE. Additionally, they noticed that a heat sink configuration without TCE had better cooling rates during the discharging cycle than one with TCE.

Pal et al., (2014), presented a thermal analysis of heat sinks with a rectangle, pin, and trapezoidal tapper fins via natural convection. According to the investigation, thermal mass, surface area, and fin design all significantly impacted heat sink performance.

Four alternative heat sink designs, including I pure PCM, (ii) PCM in a silicon matrix, (iii) PCM in a graphite matrix, and (iv) pure PCM in a system of fins, were the subject of studies by Gharbi et al., (2015). According to their observations, the heat sink with the graphite matrix achieves lower heater temperatures than the heat sink with the silicon matrix at the end of the charging cycle. They also stated that for the same fraction of copper, long copper fins could improve heat distribution into PCM more than shorter fins, allowing the component temperature to remain below the critical limit for a longer period. They also discovered that the heat sink performance is independent of the heat sink configuration during the discharging cycle. There was no significant reduction in discharging time when graphite or silicone matrix-filled PCM was used.

Fan et al. (2015) concluded that it is always appropriate to adopt composite PCMs with enhanced thermal conductivity for expedited recovery of heat during the conduction-dominated cooling (solidification) periods.

Zhu et al. (2015) discovered that during the charging cycle, filling of the metal foam to 66% of the cavity volume is more economical than that of a completely filled cavity for both the pore sizes considered. During the discharging cycle, the effect of the metal foam fill ratio was found to be negligible. Further, it was also seen that the heat sink with and without metal foam had the same rate of temperature drop in the discharging cycle.

L.W Fan et al., (2016) tested a liquid metal, i.e., a low melting point Pb-Sn-In-Bi alloy, as the phase change material (PCM) in thermal energy storage-based heat sinks against an organic PCM (1-octadecanol) with a similar melting point of 60˚C. The thermophysical properties of the two types of PCM are investigated, and it is discovered that the liquid metal is much more conductive, while both have nearly identical volumetric latent heat of fusion (215 MJ/m^3). Using the same volume of 80 mL, i.e., the same energy storage capacity, the liquid metal

outperforms the organic PCM significantly under various heating powers up to 105.3 W/cm^2. The use of liquid metal during the heating process results in a notable increase of the effective protection time to almost twice as long as it was before, as well as a reduction in the greatest overheating temperature of up to 50˚C. By utilizing the liquid metals substantially increased thermal conductivity, the cool-down duration can also be drastically reduced. These results imply that liquid metals might be a feasible PCM choice for specific applications when the volume constraint is strict and the penalty for weight growth is tolerable.

The cooling of portable electronic devices is accomplished via effective thermal management (TM) based on phase change material (PCM), according to a study by (Arshad et al.,2018). To absorb the thermal energy generated by such electronics, PCM, namely n-eicosane, is used. A no-fin heat sink (used as a reference heat sink) and four distinct configurations of the circular pin-fin heat sink with fin thicknesses of 2 mm, 3 mm, and 4 mm were also employed. Aluminum was used to make pin-fins because it is lightweight, has strong thermal conductivity, and may be used as a thermal conductivity enhancer (TCEs). To determine the optimal PCM volume, four volumetric fractions are put into pin-fin heat sinks with a constant (9%) volume fraction of TCE. At the heat sink base, a wide range of heat flux is offered, and this study reports on the impact of the fin configuration, PCM volume, latent heat phase, power densities, thermal capacity, and thermal conductance. For this experiment, three distinct critical set point temperatures (SPTs) are chosen. To demonstrate the thermal performance of passive cooling, enhancement ratios are provided against various PCM fractions. The findings indicate that the heat sink with 3 mm thick fins has the optimum operational improvement for the TM module managing the temperature of electrical devices.

CHAPTER 3

HEAT SINKS

A component called a heat sink promotes heat transfer away from a hot gadget. By enlarging the device's working surface area and the volume of low-temperature fluid that flows through it, it achieves this goal. We find a wide range of heat sink aesthetics, design, and final capabilities depending on each device's arrangement. Heat is transferred away from a critical component using a heat sink. Four simple procedures are used by almost all heat sinks to complete this task:

1. Heat is produced by the source: Any system that generates heat and needs its removal to order to operate properly can serve as this source, including:

- Friction
- Mechanical
- Electrical
- Chemical
- Nuclear
- Solar

2. Heat transfers away from the source: This process can also be aided by heat pipes, but we'll discuss those parts separately. Direct heat sink-contact applications use natural conduction to transfer heat from the source to the heat sink. The thermal conductivity of the heat sink material has an immediate effect on this procedure. The most frequent materials used in the building of heat sinks are those with high thermal conductivity, including copper and aluminium.

3. Heat distributes throughout the heat sink: As heat moves across the thermal gradient from a high temperature to a low-temperature environment, it will naturally conduct via the heat sink. This finally means that the thermal profile of the heat sink won't be constant. As a result, heat sinks frequently get hotter closer to the source and cooler farther away.

4. Heat moves away from the heat sink: This procedure depends on the heat sink's temperature gradient and working fluid, which is often air or a liquid that isn't

electrically conductive. Thermal convection and thermal diffusion are used by the working fluid as it moves over the warm heat sink's surface to transfer heat from the surface to the surrounding air. To extract heat from the heat sink, this stage once more depends on a temperature gradient. Therefore, no convection and subsequent heat removal will take place if the ambient temperature is not lower than the heat sink. The entire heat sink surface area is likewise at its most useful during this stage. A big surface area increases the region where thermal convection and diffusion can take place.

3.1 ACTIVE HEAT SINKS & PASSIVE HEAT SINKS

Heat sinks are most commonly utilized in active, passive, or hybrid configurations. Passive heat sinks rely on natural convection, which means that the airflow generated over the heat sink system is only caused by the buoyancy of hot air. These systems have the advantage of not requiring additional power sources or control mechanisms to dissipate heat from the system. However, compared to active heat sinks, passive heat sinks are less efficient at removing heat from a system.

Fig.3.1.3 Passive heat sink

Forced air is used by active heat sinks to promote fluid flow across the heated area. Most frequently, forced air is produced by a fan, blower, or even by the movement of the entire thing. For example, the engine of a motorcycle is cooled by air passing along heat sink fins built into the engine. Your personal computer's fan coming on

as it gets warm is an example of a fan providing forced air across a heat sink. As more unheated air is forced across the heat sink surface by the fan, the total thermal gradient across the heat sink system increases, allowing more heat to escape the system as a whole.

Fig.3.1.4 Active heat sink

Aspects of passive and active heat sinks are combined in hybrid heat sinks. These setups are less frequent and frequently depend on control systems to cool the system in accordance with temperature requirements. The forced air source is inactive when the system is operating at lower temperatures, just passively cooling the system. The active cooling mechanism activates to boost the heat sink system's cooling capacity whenever the source reaches greater temperatures.

CHAPTER 4

PHASE CHANGE MATERIAL-BASED HEAT SINK

Standard heat sinks for electronics cooling act as heat exchangers, transferring heat from the electronics to air or coolant. The only heat sinks that serve as a (temporary) heat sink are made of phase change material (PCM). They are becoming more prevalent in the field of thermal management to address thermal issues in systems where active solutions are impractical. A PCM heat sink is capable of absorbing the generated waste heat when there is nowhere for it to be dissipated by electric components.

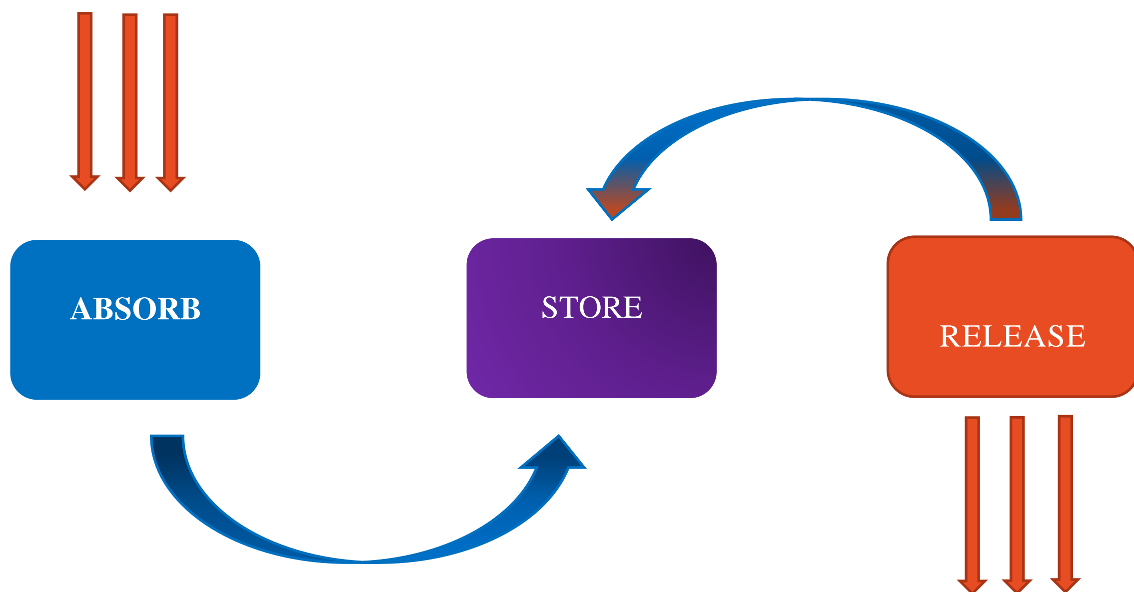

Fig.4.5 Working of PCM

By transitioning from a solid to a liquid phase, phase change materials (PCMs) can store thermal energy. This is beneficial since the energy stored by the specific heat throughout a representative 10°C shift in temperature is at least 1-2 orders of magnitude more than the latent heat from melting or freezing. Electronics thermal management PCM applications include:

- Temperature stabilization during pulsed operation.
- When a suitable heat sink is not available, there is a short-term thermal storage option.

- Protection from malfunction when the cooling system is momentarily unavailable and there are coolant interruptions.

Any substance that needs a lot of energy to change phases is referred to as PCM. Latent heat of fusion is the term used to describe the energy needed to change from a solid to a liquid state. High latent heat of fusion materials can store a substantial amount of heat during a phase transition while keeping their melting point temperature relatively constant. For electronics cooling applications with transient loading, this feature is helpful. While heat is being generated during transient operation, the thermal energy can be stored in the PCM without considerably raising the temperature of the source.

Fig.4.5 demonstrates the thermal advantage of utilizing a phase-change material for transient loads. The temperature increase per unit of absorbed energy is represented by the slope. With practically any temperature change in temperature, a significant quantity of energy is stored during the melt. In applications with ergonomic requirements, a constant temperature is especially tempting. However, it is advantageous in many other applications to prevent component failure during transient power spikes.

4.1 SENSIBLE HEAT STORAGE AND LATENT HEAT STORAGE

Sensible heat is the most typical kind of thermal energy storage. The temperature of the storage medium rises as a result of heat being transferred to it, as depicted in the picture below. Hot water storage for residential heating and hot water is a typical illustration.

Large amounts of heat or cold can be stored in solids and liquids during the phase shift process caused by melting and solidification. A tiny volume change, often less than 10%, results from melting. The pressure barely changes if the material can fit in the container in its liquid state. As a result, the storage material melts and solidifies at a constant temperature. The heat from melting is transferred to the storage substance and keeps it at a steady temperature. This is the phase change temperature. Further transfer of heat after melting results in sensible heat storage. The heat supplied upon melting is latent heat, and the process is latent heat storage.

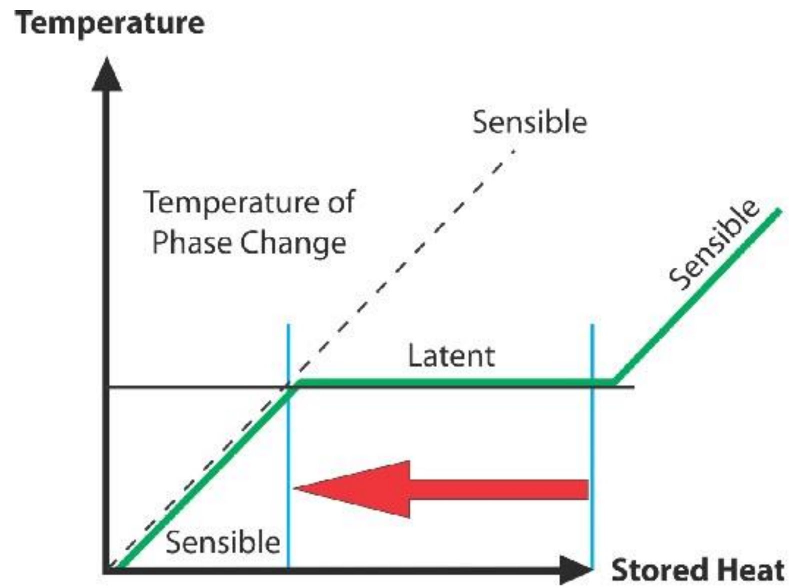

Fig.4.1.6 Sensible Heat vs. Latent Heat

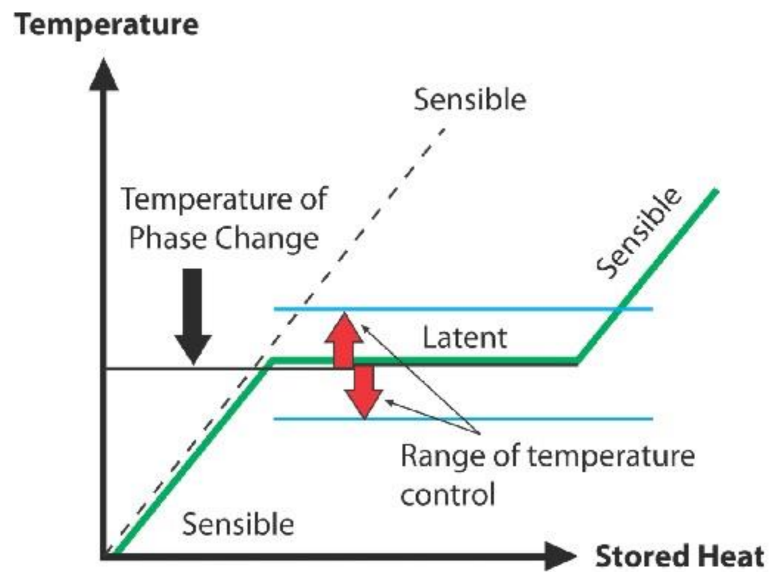

Fig.4.1.7 Temperature Control During Phase Change Energy Storage

Sensible, $Q_{sensible}$ (kJ) and latent heat, Q_{latent} (kJ) are represented in Eq. 1 and 2, respectively.

$Q_{sensible} = m \times Cp \times \Delta T$ 4.1.1

$Q_{latent} = m \times h_l$ 4.1.2

where m = mass (kg); Cp = specific heat (kJ/kg˚C); ΔT = Temperature difference (˚C); h_l = specific latent heat (kJ/kg)

4.2 CLASSIFICATION OF PCM

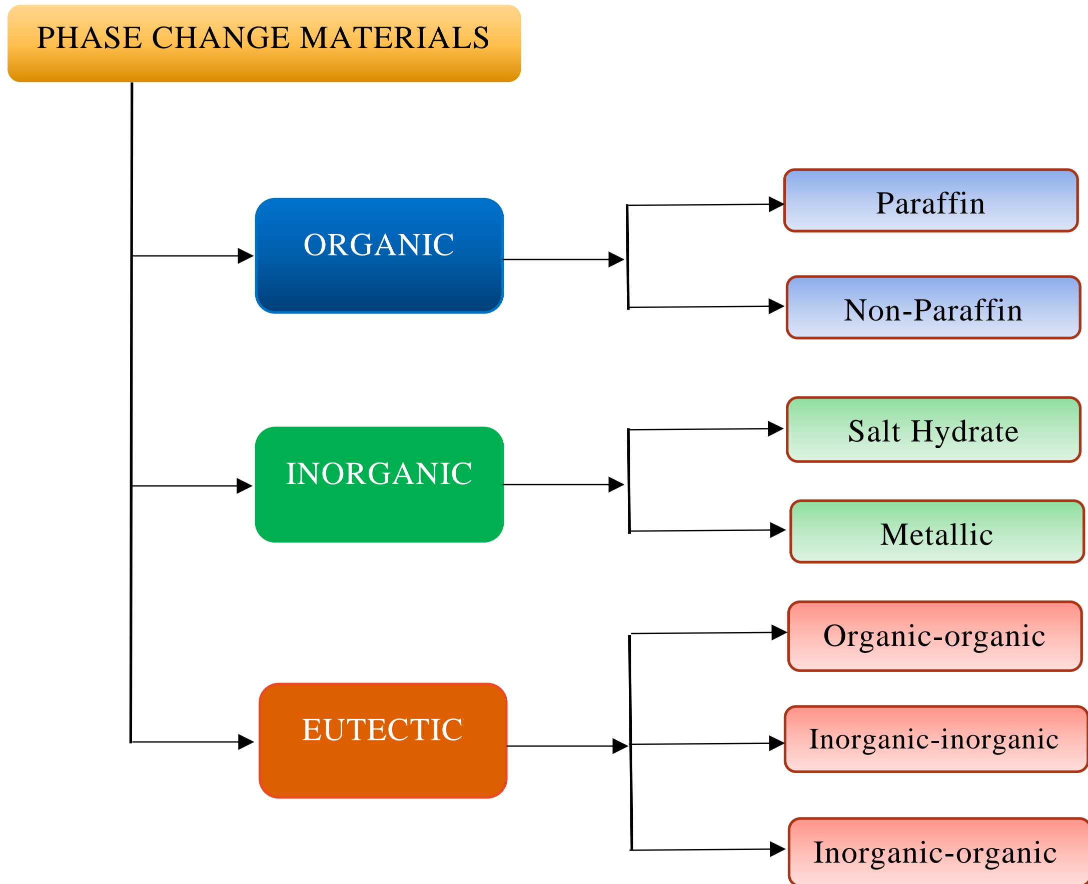

Fig.4.2.8 Classification of PCM

Inorganic: Engineered hydrated salt solutions created from natural salts and water are known as inorganic PCM. To get the necessary phase transition temperature, the salts' chemical makeup is changed in the combination. Salt separation and supercooling, which are features of hydrated salt PCM, are reduced by special nucleating agents that have been introduced to the combination. Salt Hydrates are safe, non-flammable, and cost-effective.

Bio-based: PCM are organic substances that are fatty acids that are found in nature, including vegetable oil. Their phase change temperature varies according to their chemical components. These goods have an endless lifespan and are non-corrosive and non-toxic. They can be costly as well as flammable at high temperatures.

Natural petroleum byproducts known as organic PCM have a certain phase transition temperature. These products may not be widely available because they are produced by large petrochemical corporations. They might be costly, combustible, and toxic. They have endless lifespans, and their cost fluctuates in response to variations in the price of crude oil around the world.

Paraffin and non-paraffin organics are ideal phase change materials because they melt and freeze uniformly (i.e., have the same composition before and after freezing) and can therefore be used for applications requiring material stability through several cycles. These materials' thermal conductivity, which is typically 0.2 W/m-K, is their main flaw. Alkanes, or saturated hydrocarbons, such as paraffin, are inert phase change substances. Other than fatty acids, non-paraffin organic compounds are mildly corrosive and more expensive than paraffin materials.

4.3 PROPERTIES OF PCM

The type of PCM that can be utilized depends on the melt temperature and the application. Paraffin waxes and non-paraffin organics are a good option for the majority of electronics applications since they are reasonably priced and stable through numerous temperature cycles. Metals and salts (non-hydrated) can be employed for high-temperature applications.

The phase change material should possess the following thermodynamic properties:

- Melting temperature in the desired operating temperature range
- High latent heat of fusion per unit volume
- High specific heat, high density, and low thermal conductivity
- Small volume changes on phase transformation and small vapor pressure at operating temperatures to reduce the containment problem
- Congruent melting

Kinetic properties:

- High nucleation rate to avoid supercooling of the liquid phase.
- High rate of crystal growth, so that the system can meet demands of heat recovery from the storage system.

Chemical properties:

- Chemical stability
- Complete reversible freeze/melt cycle
- No degradation after a large number of freeze/melt cycle
- Non-corrosiveness, non-toxic, non-flammable, and non-explosive materials

Table 4.3.1 Properties of PCM

Property or characteristics	Paraffin wax	Non-paraffin organics	Hydrated salts	Metals	Salts
Heat of fusion	High	High	High	Medium	Very high
Thermal conductivity (W/mK)	-0.2	-0.2	-0.5-10	Very high	-0.5-10
Volumetric storage capacity (MJ/m^3)	-190	-150	-300	-840	-600
Melt temperature (˚C)	-20-100+	5-120+	0-140+	150-800+	200-800+
Latent heat(kJ/kg)	200-280	90-250	60-300	25-300	150-1000+
Corrosive	Noncorrosive	Mildly corrosive	Relatively corrosive	Varies	Corrosive
Thermal cycling	Stable	High heat can cause dissolving	Stable but need caution	Stable	Stable but need caution
Weight	Medium	Medium	Light	Heavy	Light

4.4 ADVANTAGES OF PHASE CHANGE ENERGY STORAGE

- During the application process thermal energy is stored at the temperature of the process.
- Store thermal energy as latent heat which allows higher thermal energy storage capacity per unit weight or material without any temperature change.
- Store thermal energy from the thermal or electrical energy source and use it when needed.
- Stored thermal energy is rechargeable and portable.

4.5 ECONOMICAL & ENVIRONMENTAL BENEFITS

- For the purpose of facility heating and cooling, store thermal energy from nature. Carbon footprint is decreased by reduced energy usage.
- By storing thermal energy during off-peak hours and using it during peak demand hours, you can reduce your energy costs and assist in balancing the grid's load.
- Shifting heating and cooling loads lessens the equipment's peak-time stress, which lowers operating and maintenance expenses.
- Because of this technology, HVAC equipment is now sized for normal loads rather than peak loads.

When a suitable heat sink is not available, PCM heat sinks are utilized for a variety of electronics cooling applications, including temperature stability during pulsed operation, short-term thermal storage, and failure protection in cases of coolant loss, to mention a few. A PCM heat sink can decrease system size, cost, maintenance, and power need if the thermal storage capacity of the PCM is appropriate for an application.

The precise needs of the application will determine the phase change material and enclosure that are used. The most common materials employed are paraffin waxes and non-paraffin organics, but metals and hydrated or non-hydrated salts can also be used in some specialized applications. PCM heat sink design challenges include the low thermal conductivity of most PCMs. Thermal enhancement such as fin or heat pipes are generally used to improve thermal conductivity.

4.6 THERMAL CONDUCTIVITY ENHANCERS

The main drawback of the PCM is the low thermal conductivity. To enhance this thermal conductivity enhancer are used. Fins, metal foams, and baffles are the commonly used TCEs.

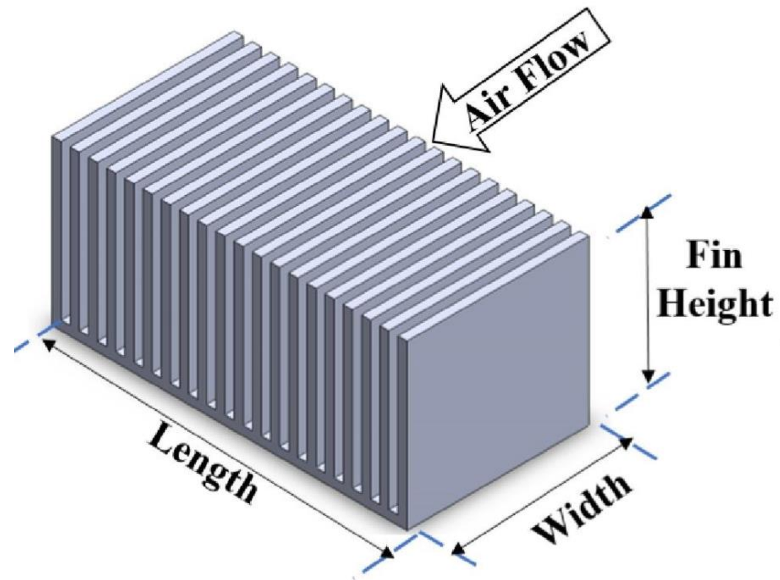

Fig.4.6.9 Rectangular heat sink [Ali Elghool and Firdaus Basrawi et al. (2017)]

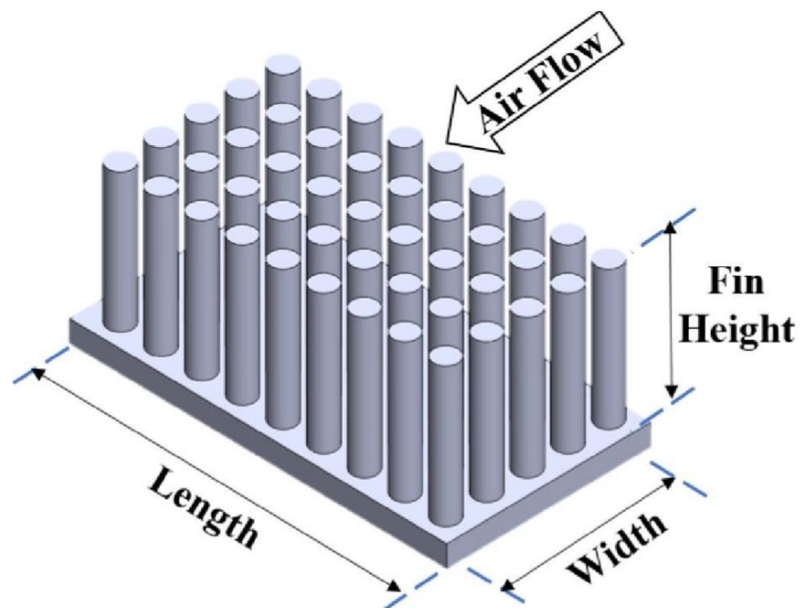

Fig.4.6.10 Pin fin heat sink [Ali Elghool and Firdaus Basrawi et al. (2017)]

CHAPTER 5

COMPUTATIONAL FLUID DYNAMICS

5.1 INTRODUCTION TO CFD

Computational Fluid Dynamics (CFD) is one of the branches of fluid mechanics that uses numerical methods and algorithms to solve and analyze problems that involve fluid flows. Computers are used to perform the millions of calculations required to simulate the interaction of fluids and gases with the complex surfaces used in engineering. CFD predicts what will happen, quantitatively, when fluid flow, often with the complications of;

- Simultaneous flow of heat
- Mass transfer
- Phase change
- Chemical reaction
- Mechanical movement
- Stress and displacement of immersed solids

5.2 CFD APPLICATIONS

- Aerodynamics of aircraft and vehicles; lift and drag
- Hydrodynamics of ships
- Power plants; combustion in IC engines and gas turbines
- Turbo machinery; flow inside rotating passages
- Metrology; weather predictions
- External and internal environment of buildings; wind loading

5.3 NUMERICAL METHODS USED IN CFD

The methods used in CFD are;

- Finite Difference Method (FDM)
- Finite Element Method (FEM)
- Finite Volume Method (FVM)

5.3.1 Finite Difference Method (FDM)

The simplest numerical technique to apply for the solution of the heat/diffusion equation is the finite difference method. The basic idea behind the method is to replace the various derivatives appearing in the mathematical formulation of the problem by suitable approximations on finite difference mesh of nodes. The simplest derivation of finite difference formulae makes use of Taylor series. The final set of linear algebraic equations is solved by any numerical techniques.

5.3.2 Finite Element Method (FEM)

The finite element method subdivides the calculation domain into element, such as triangular rectangles, tetrahedral or rectangular parallelepipeds elements. These elements are considered to inter connected at specified joints called nodes. Here the variation of field variable is inside a finite element can be approximated by a simple function. These approximating functions are defined in terms of the values of the field variables at the nodes. When field equations are written for whole continuum the new unknowns are at the nodal points. By solving the field equations, which are generally in the form of matrix equations, the node values of the field's variables will be known. Once these are known, approximating functions define the field variable through the assemblage of elements.

5.3.3 Finite Volume Method (FVM)

This is the classical or standard approach used most often in commercial software and research coded. An alternative discretization method is based on the idea of regarding the computation domain as subdivided into a collection of finite volumes. In this view, each finite volume is represented by a line in 1D, an area in 2D and volume in 3D. Nodes, located inside each finite volume, become the locus of computational values. In rectangular Cartesian coordinates in 2D the simplest finite volumes are rectangles. For each node, the rectangle faces are formed by drawing perpendiculars through the midpoints between contiguous nodes. Discretization equations are obtained by integrating the original partial differential equation over the span of each finite volume. This method is easily extended to

nonlinear problems. The solutions of the algebraic equations are obtained by iterative methods.

One advantage of this method over FDM is that it does not require a structured mesh - although a structured mesh can be used. The FVM can solve problems on irregular geometries. Furthermore, one advantage of this method over FEM is that it can conserve the variables on a coarse mesh easily. This is an important characteristic of the fluid problem.

5.4 ADVANTAGES OF CFD OVER EXPERIMENT METHODS

CFD analysis results in a substantial reduction of lead time and cost of new design. It is possible to study systems where controlled experiments are difficult or impossible to perform (e.g., very large systems) and also study systems under hazardous conditions. It provides practically unlimited level of detailed results.

The variable cost of an experiment, in terms of facility hire or man-hour costs, is proportional to the number of data points and the number of configurations tested. In contrast CFD codes can produce extremely large volumes of results at virtually no added expense and it is very cheap to to optimize equipment performance.

5.5 WORKING OF A CFD CODE

CFD codes are structured around the numerical algorithms that can tackle fluid flow problems. In order to provide perform parametric studies, for instance easy access to the solving power all commercial CFD packages (Phoenics, Flow3D, Star CD) include sophisticated user interfaces to input problem parameters and to examine the results. All codes contain 3 main elements.

- Pre-Processor
- Solver
- Post-Processor

5.5.1 Pre-processor

Pre-processing consists of the input of a flow problem to a CFD program by means of an operator friendly interface and the subsequent transformation of this input into a form suitable for use by the solver. The user activities at the pre-processing stage involve,

- Definition of the geometry of the region of interests: the computational domain
- Grid generation: the sub-division of the domain into a number of smaller, non- overlapping sub-domains known as grid of cells or mesh (control volumes or elements).
- Selection of the physical and chemical phenomena that need to be modelled.
- Definition of fluid properties.
- Specification of appropriate boundary conditions at cells which coincide with or touch the domain boundary.

The solution to a flow problem is defined at the nodes inside each cell. The accuracy of a CFD solution is governed by the number of cells in each grid.

5.5.2 Solver

There are three distinct streams of numerical solution techniques: finite difference, finite element and spectral methods. In outline the numerical methods that form the basis of the solver perform the following steps.

- Approximation of the unknown flow variables by means of simple functions.
- Discretization by substitution of the approximations into the governing flow equations and subsequent mathematical manipulations.
- Solution of the algebraic equations.

The main differences between the three separate streams are associated with the way in which the flow variables are approximated and with the discretization processes.

5.5.3 Post-processor

As in pre-processing a huge amount of development work has been recently taken place in the post-processing field. The increased popularity of engineering work stations, many of which have outstanding graphics capabilities, the leading CFD packages are now equipped with versatile data visualization tools. These include,

- Domain geometry and grid display
- Vector plots
- Line and shaded contour plots
- 2D and 3D surface plots
- Particle tracking
- View manipulation (translation, rotation, scaling etc.)
- Colour postscript output.

5.6 PROBLEM SOLVING WITH CFD

In solving fluid flow problems, we need to be aware that the underlying physics is complex and the results generated by a CFD code are at best as good as the physics and chemistry embedded in it and at worst as its operator. Prior to setting up and running a CFD simulation there is a stage of identification and formulation of the flow problem in terms of the physical and chemical phenomena that need to be considered. Over 50% of time spent in industry on a CFD project is devoted to the definition of the domain geometry and grid generation.

5.7 COMPUTATIONAL FLUID DYNAMICS SIMULATION

The design, scale-up, and running of unit operations in chemical process industries rely heavily upon empiricism and correlations of overall parameters for non-ideal or non-equilibrium conditions. Many equipment designs in use are based on the experience of experts applying rules of thumb, resembling art more than science. Processes that are sensitive to local phenomena and reactant concentrations are often difficult to design or scale up, because the design correlations do not take local effects into account. Non-idealises introduced by scaling up of lab or pilot scale equipment are difficult, if not impossible to predict accurately.

Researchers, equipment designers, and process engineers are increasingly using computational fluid dynamics (CFD) to analyse the flow and performance of process equipment, such as chemical reactors, stirred tanks, fluidized beds, cyclones, combustion systems, spray dryers, pipeline arrays, heat exchangers and other equipment. CFD allows for in depth analysis of the fluid mechanics, local effects, and chemistry in these types of equipment such as turbulence and combustion. CFD can be used when design correlations or experimental data are not available. It provides comprehensive data that are not easily obtainable from experimental tests. It highlights the root cause, not just the effect and many 'what if' scenarios can often be analysed in a short time. This method reduces scale-up problems, because the models are based on the fundamental physics and are scale-independent.

CFD is basically the science of predicting fluid flow, heat transfer, mass transfer, chemical reactions, and related phenomena by solving the mathematical equations that govern these processes using numerical algorithm. It is the merger of the classical branches of theoretical and experimental science, with the infusion of the modern element of numerical computation. The results of CFD analyses are relevant engineering data used in conceptual studies of new designs, detailed product development, troubleshooting, and redesign. In many cases, CFD results in better insight, improved performance, better reliability, more confident scale-up, improved product consistency, and higher plant productivity.

The progress of CFD during the last fifty years has been extraordinary. Much of this progress has been driven by the phenomenal increases in digital computing speed. The continual and exponential increase in computing power, improved physical models in many CFD codes, and better user interfaces now enables non-experts to use CFD as a design tool on day-to-day basis. As a consequence, CFD has progressed from the domain of mainframe to the high-end engineering workstation and even to laptop PCs. This power of digital computing has transformed research and engineering especially in fluid mechanics, just as it has in virtually all fields of human endeavours.

5.8 PHASES OF MODELLING AND SIMULATION

There has been a long history of efforts to establish the basic concepts and terminology in modelling and computer simulation. The identification of the fundamental issues and debates began two decades ago in the operation research community, long before there was such concern in the CFD community. The term model, modelling, and simulation are used in a wide range of disciplines. Consequently, these terms have a range of meanings that are both context-specific and discipline-specific. Model is a representation of a physical system or process intended to enhance our ability to understand, predict, or control its behaviour. Modelling is the process of construction or modification of a model. Simulation is the exercise or use of a model.

The basic phases of modelling and simulation have been identified by operation research community. Figure 3.1 shows these basic phases and processes. It identifies two types of models: a conceptual model and a computer model. The conceptual model is composed of all the information, mathematical modelling data, and mathematical equations that describe the physical system or process of interest. The conceptual model is produced by analysis and observations of the physical system. In CFD, the conceptual model is dominated by partial differential equations. The computer model is an operational computer program that implements a conceptual model. Modern terminology refers to the computer model as computer code.

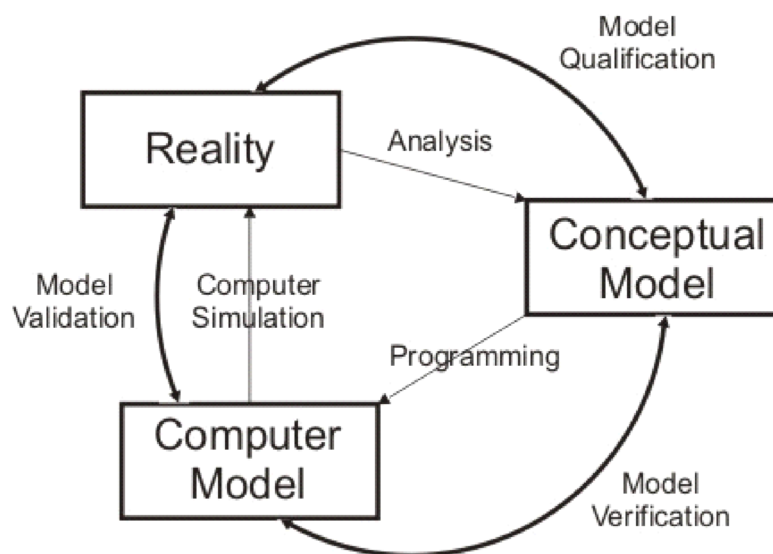

Fig.5.8.11 Phases of modelling and simulation

Although CFD simulations are widely conducted in industry, government and academia, there is presently little agreement on procedures for assessing their capability. There is no fixed level of credibility or accuracy that is applicable to all CFD simulations. The accuracy level required of simulations depends on the purposes for which the simulations are intended to be used.

The two main principles that are necessary for assessing credibility are verification and validation. Verification is the process of determining if a computational simulation accurately represents the conceptual description of the model and the solution to the model, but no claim is made of the relationship of the simulation to real world. Validation is the process of determining if a computational simulation accurately represents the real world from the perspective of the intended uses of the model. The definition of verification and validation also stresses the evaluation of accuracy. In verification activities, accuracy is generally measured with the respect to benchmark solutions of simplified model problems. In validation activities, accuracy is measured with respect to experimental data, which represent reality.

Uncertainty and error can be considered as the broad categories that are normally associated with the loss in accuracy in modelling and simulation. Uncertainty is defined as a potential deficiency in any phase or activity of the modelling process that is due to lack of knowledge.

Lack of knowledge is commonly caused by incomplete knowledge of a physical characteristic or parameter. Lack of knowledge can also be caused by the complexity of a physical process, for example in the case turbulent combustion. Error is defined as a recognizable deficiency in any phase or activity of modelling and simulation that is not due to the lack of knowledge. Error can be categorized as either acknowledged or unacknowledged. Examples of acknowledged errors are round- off error in a digital computer and physical approximations made to simplify the modelling of a physical process. Unacknowledged errors include blunders and mistakes such as programming errors.

In CFD simulations, there are four predominant sources of error, namely insufficient spatial discretization convergence, insufficient temporal discretization convergence, lack of iterative convergence, and computer programming. The most important activity in verification testing is to systematically refining the grid size and the

time step. The objective of this activity is to estimate the discretization error of numerical solution. As the grid size and time step approach zero, the discretization error should asymptotically approach zero. In verification activities, comparing a computational solution to a highly accurate solution is the most accurate and reliable way to quantitatively measure the error in the computational solution. However highly accurate solutions are known for a relatively small number of simplified problems. These highly accurate solutions can be classified into three types: analytical solutions, benchmark numerical solutions to ordinary differential, and benchmark numerical solutions to partial differential equations.

5.9 CFD CALCULATION

CFD is applied by first dividing or discretizing the geometry of interest into a number of computational cells. Discretization is the method of approximating the differential equations by a system of algebraic equations for the variables at some set of discrete locations in space and time. The discrete locations are referred to as the grid or the mesh.

The continuous information from the exact solution of the Navier-Stokes partial differential equations is now replaced with discrete values. The number of cells can vary from a few thousands for a simple problem to millions for very large and complicated ones. Cells have a variety of shapes. Triangular and quadrilateral cells are generally used in 2D problems. For 3D problems, hexahedral, tetrahedral, pyramidal, and prismatic shaped cells can be used.

In the past, CFD codes required the use of structured grids containing one cell type, such as brick-shaped hexahedral elements, in which the cells were positioned in regular pattern. Current codes allow cells to be located in an irregular, unstructured pattern, giving much greater geometric flexibility. Additionally, a good CFD code can accept grids consisting of a combination of different cell types, or hybrid grids, to address complex geometries, providing flexibility to the CFD analyst. Geometries are often created using computer aided design (CAD) software. The geometry, either a wire frame or solid model is exported to the grid-generation software program to create the CFD quality grid. A few packages have combined both functions of CAD geometry creation and mesh generation into a single interface. With the grid created, the boundary conditions such as pressures, velocities, mass flows, and scalars specified, and physical properties defined, the CFD

calculations can start. The CFD codes will solve the appropriate conservation equations for all grid cells using iterative procedure. Typical chemical process applications involve solving for: mass conservation (using a continuity equation), momentum (using Navier Stokes equations), enthalpy, turbulent kinetic energy, turbulent energy dissipation rate, chemical species concentrations, local reaction rates, and local volume fractions for multiphase problems.

There are many commercial CFD packages for modelling and analysing system involving fluid flow, heat transfer and associated phenomena such as chemical reaction. Some popular CFD packages include: FLUENT, CFX, PHOENICS and ANSYS. All these commercial CFD codes contain three main elements: Pre- processor, Solver and Post-processor. This study concentrates on the use of ANSYS 19.2 software package to simulate the flow and mixing behaviour especially for chemical and thermal industrial applications.

CHAPTER 6

NUMERICAL STUDY ON HEAT TRANSFER

6.1 INTRODUCTION

The ANSYS FLUENT R19.2 CFD software was used for the simulations. Computational Fluid Dynamics (CFD) is the science of predicting fluid flow, heat transfer, mass transfer, chemical reactions, and related phenomena by solving the mathematical equations which govern these processes using a numerical process.

The result of CFD analysis is relevant engineering data used in: conceptual studies of new designs detailed product development troubleshooting redesign CFD analysis complements testing and experimentation. Reduces the total effort required in the laboratory.

The simulation procedure started with pre-processing. The geometry was drawn in the design modeler by using the sketching option with proper dimension. Boolean, extrusion (add frozen, add material), and the pattern was the major operations to get the required geometry. The body of the heat sink was made of aluminium and it takes a solid body, PCM inside the heat sink was taken as fluid. The computational mesh was generated using orthogonal elements. And also edge sizing is done for a more precise and accurate mesh. After meshing suitable naming is given to the meshed geometry. SIMPLE algorithm was used. This study was considered transient because the melting of PCM was a time-dependent process.

6.2 VALIDATION OF EXPERIMENTAL DATA

The numerical models are created with the same dimensions of heat sink configuration mentioned in the experimental data Arshad et al., (2018). The rubber pad for the heat sink bottom, silicon rubber gaskets, and Perspex sheet are not modeled in the numerical simulations. The pressure-velocity coupling is handled by the SIMPLE (Semi-Implicit Method for Pressure Linked Equations) algorithm, while the pressure correction is handled by the PRESTO (Pressure Staggering Option) scheme. The second-order upwind scheme is used for discretizing both the momentum and the energy equations. The under relaxation value factors are set at

0.3, 1.0, 0.7, and 0.9 for pressure, density, momentum, and liquid fraction, respectively. The second-order implicit method is used for transient formulation.

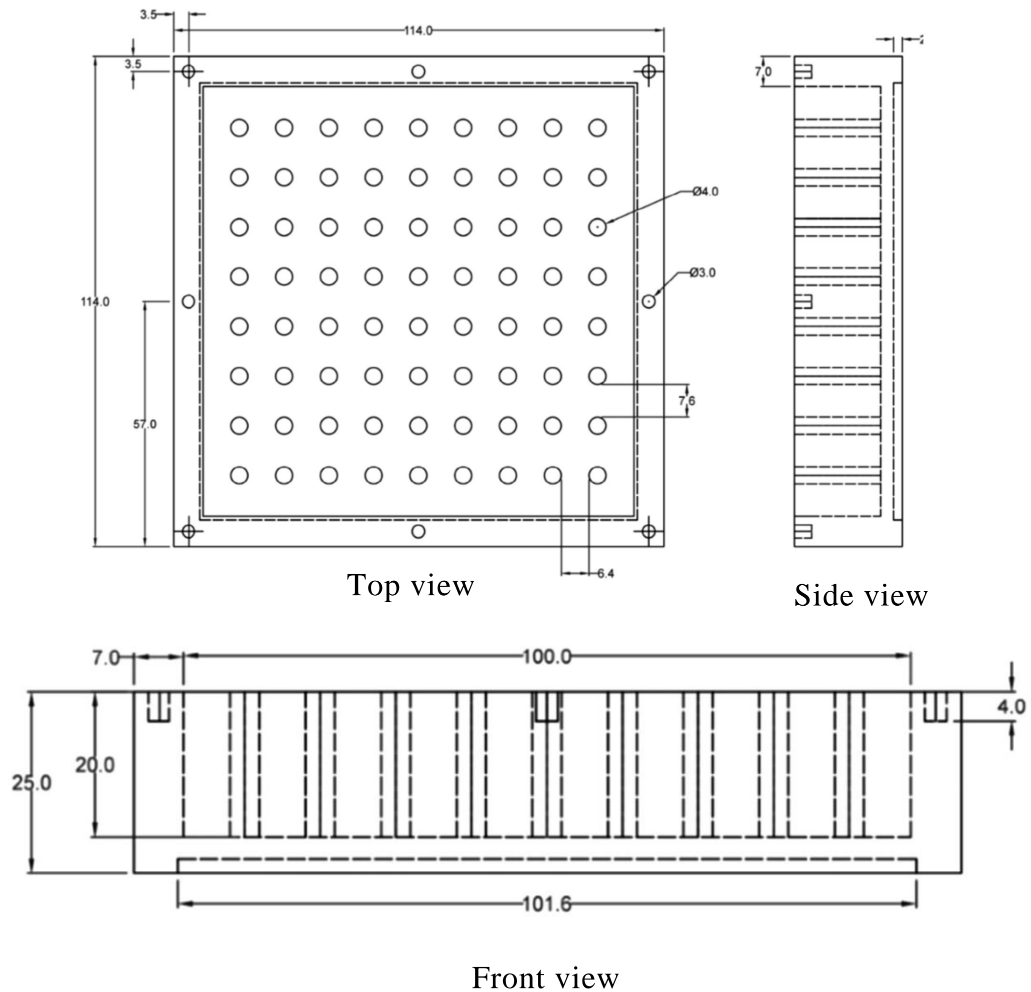

Fig.6.2.12 Dimensions of 4 mm thick pin-fin heat sink [Arshad, et al. (2018)]

The pin fin heat sink is drawn as per the dimension mentioned above. The geometry is drawn in ANSYS Fluent design modeler and gets the computational domain Fig.6.2.1.13.

6.2.1 Computational Domain

Experimental research on the heat sink's performance under different power levels of 2000W, 2400W, and 2800W by Arshad et al. was conducted [30]. The heat sink had external measurements of 114*114*25 mm^3. The cavity was 100 mm^3*100

mm^3*20 mm^3. The identical beginning and boundary conditions used in Arshad et al. are used in this study to numerically model a heat sink with the same dimensions.

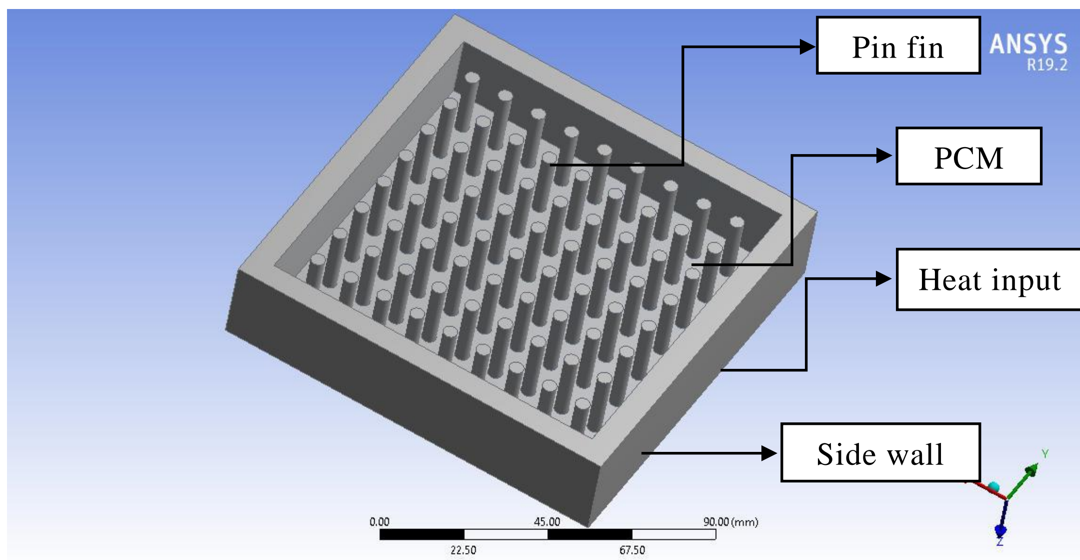

Fig.6.2.1.13 Geometry of 4 mm thick pin fin PCM-based heat sink

Geometrical Details

- Base Size = 114*114mm
- Fin Height = 20 mm
- Fin diameter = 4mm
- No Of Fins = 72
- Side wall Thick = 25 mm

6.2.2 Mesh Domain of Pin-fin heat sink

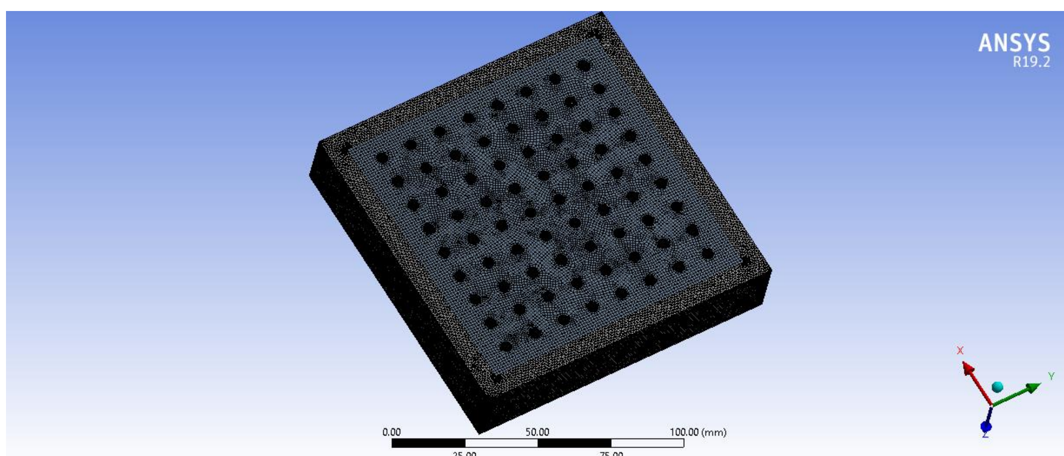

Fig.6.2.2.14 Meshing of heat sink

Grid independence studies are performed for the heat sink configuration to decide on the number of mesh elements required for the numerical simulations. The heat sink configuration is tested for coarse, medium, and fine grids. For the heat sink configuration, the number of mesh elements considered is coarse, medium, and fine. A constant heat input of 2000W/m^2 is applied at the bottom of the heat sink for 4000s. The numerical investigations are performed for a volumetric fraction of 0.9. The insulated boundary condition is applied to all the walls of the heat sink. The timestep value is 0.01s, respectively. The temperatures attained by the heater surface at different time instances for these mesh elements are plotted in Fig.6.2.2.15. From the results, it is evident that 3104418 (fine mesh) mesh elements and the number of nodes 933479 are sufficient to carry out further numerical simulations. The same procedure is followed for the different heat sink configurations of pin fin diameter, and the number of mesh elements is obtained.

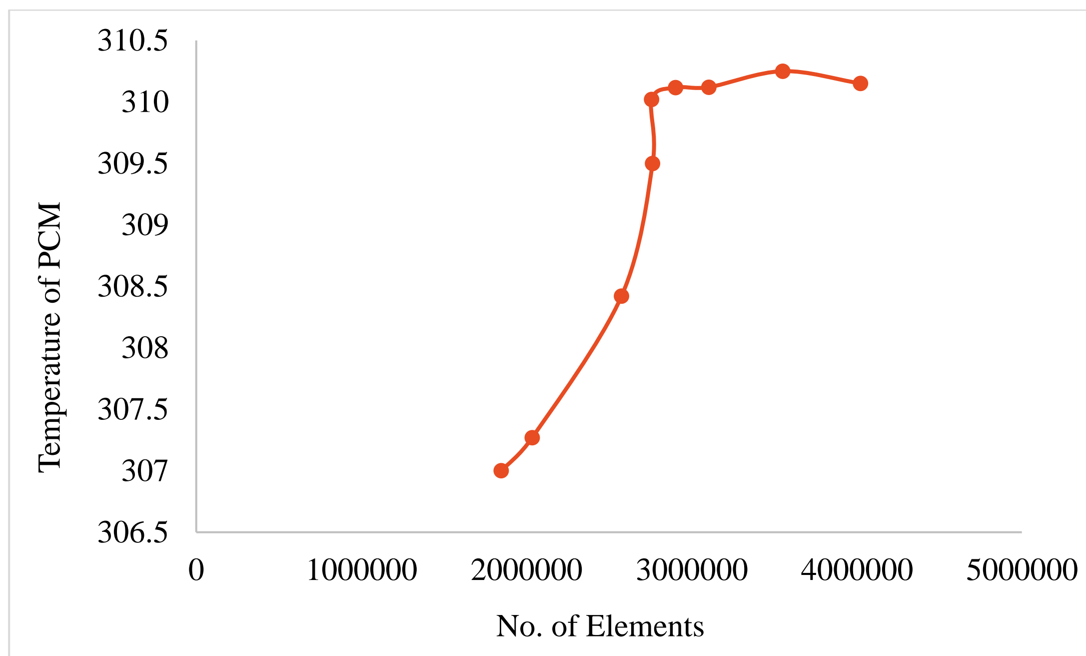

Fig.6.2.2.15 Grid independence study

6.2.3 Initial and Boundary Conditions

Although the ambient conditions are the same for both the heat sink configurations, i.e. For different pin fin diameters, during charging and discharging cycles, the performance of both heat sinks is different because of the presence of the PCM and its flow physics. The flow physics of the PCM during charging and

discharging cycles is difficult to analyze using experimental results alone, without any visualization. The numerical simulations facilitate understanding and visualization of the PCM's melting and solidification processes. The numerical simulations are carried out with the same initial and boundary conditions of experimental investigations mentioned in Arshad et al., (2018).

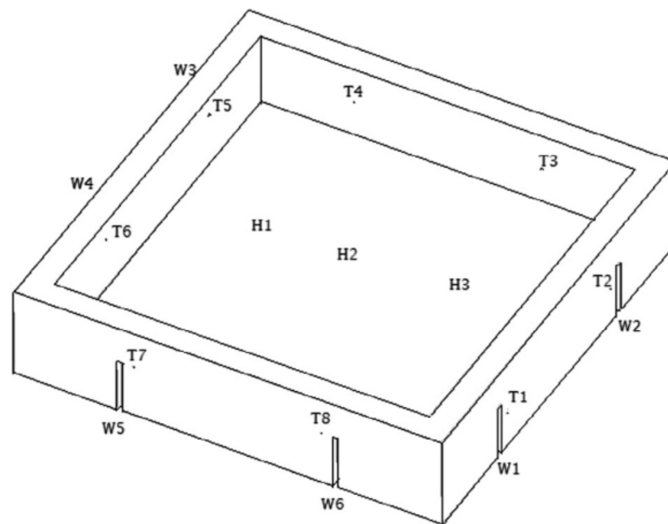

Fig.6.2.3.16 Positions of thermocouples on a heat sink [Arshad, et al. (2018)]

Since PCM dynamics is of primary concern, the temperature-time history of the walls of the heat sinks measured using the thermocouples T1, T2, T3, T4, T5, and T6 (Fig.5.2.3.13) in the experimental investigations are imposed directly as a time-varying temperature boundary condition on the walls of the numerical model for the respective heat sink configurations in the numerical simulations. The aluminum and the PCM domains are initialized at 18˚C. During the charging cycle, for the numerical model, the heat input at the heater surface is set at 2000W/m^2. Configurations of the circular pin-fin heat sink with fin thickness of 2mm, 3 mm, and 4 mm and no fin were adopted for the numerical study.

The selection of PCM is substantially the key factor for designing a heat storage module as its melting temperature should be lower than the maximum temperature at operating conditions. The specific heat capacity and latent heat of fusion must be high, especially on the volumetric basis which eventually reduces the size of the heat storage module. High density additionally favours the smaller storage size. To avoid containment issues of PCM, the volume changes while phase

transition and vapor pressure at operating temperature should be low. The chemical stability of PCM enhances the selection for repeating mode of device and it should be material compatible and non-toxic. N-eicosane (used in the present study) is used as PCM with a melting temperature of 36.5˚C (Sigma Alderich, USA) which is in the range of operating temperature of most portable handheld electronic devices. Furthermore, the maximum operating temperature of any electronic device should be higher than the melting temperature of employed PCM for thermal management. N-eicosane has a high latent heat of fusion of 237.400 J/kg which ensures a constant phase change temperature and enhances the operation time of electronic packages. The properties of n-eicosane are given in the table.

Table 6.2.3.2 Properties of n-eicosane.

Name of PCM	Thermal conductivity (W/mK)	Specific heat (kJ/kg K)	Latent heat (kJ/kg)	Melting point(˚C)	Density (kg/m^3)
n-eicosane	0.39 (solid) 0.157 (liquid)	1.9 (solid) 2.2 (liquid)	237.4	36.5	810 (solid) 770 (liquid)

Four different volume fractions of PCM (ψ=0, ψ=0.3, ψ=0.6, ψ=0.9) are adopted for each configuration of the heat sink to examine the effect of PCM amount on the thermal performance of PCM-based pin-fin heat sink. A wide range of heat flux (0.8 kW/m^2 to 2.8 kW/m^2) with a difference of 0.4 kW/m^2 is maintained with an input power source provided at the heat sink base and the effect of fin configurations, volume fractions, the effect of heat flux, and Time-temperature distribution for different pin fin thickness heat sink are validated.

6.3 NUMERICAL STUDY OF HEAT SINK WITH BAFFLES AND WITHOUT BAFFLES

The numerical simulation with and without baffles is the second goal. By improving thermal conductivity, baffles expand the heat sink's surface area. Increase heat transfer as well. The TCEs increase the charging time of the PCM. The purpose of this study was to compare the effectiveness of with baffles and those without. The charging cycle and the discharging cycle are the two working cycles that make up a conventional heat sink. The charging cycle is the time frame in which the heat sink absorbs and stores the heat.

The discharging cycle is the period in which the heat sink releases the heated air into the surrounding environment. To allow for continued use of the electronic gadgets for extended periods of time, the charging time should be as high as possible.

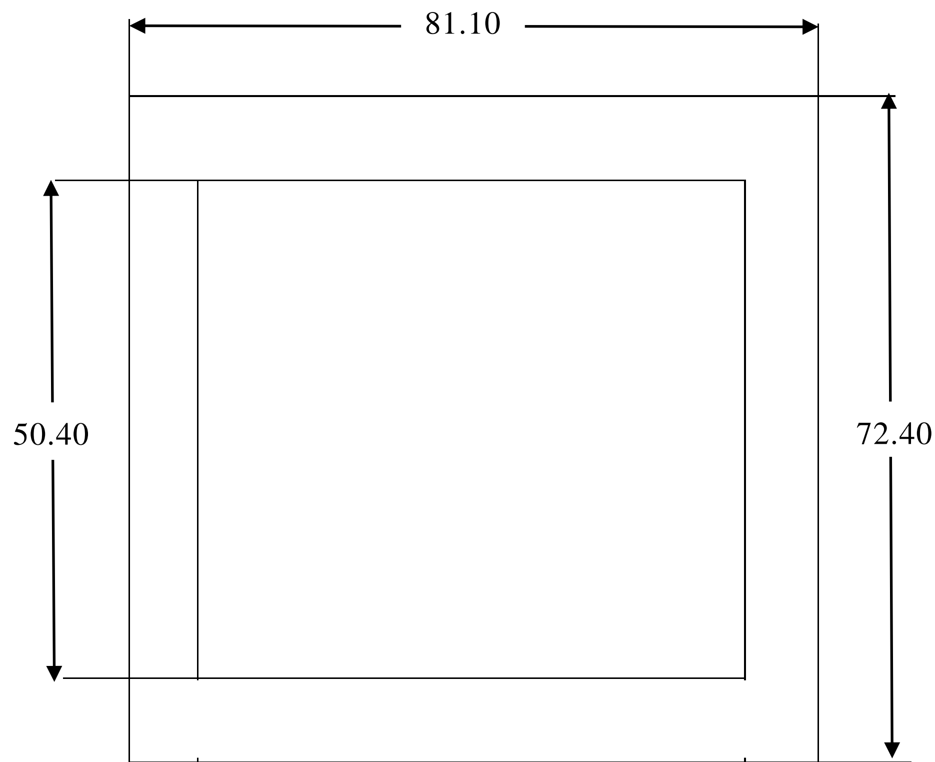

Fig.6.3.17 Dimensions of heat sink without baffles

The discharging time should be as low as possible to prepare the heat sink ready for upcoming heat loads in a periodic on-off duty cycle, which is likely to be the norm rather than the exception.

The merit of a PCM-based heat sink is the possibility of high charging time and lower discharging time. All dimensions are in mm. Dimensions of the heat sink geometry were selected from papers and provided an additional structure called baffles inside. The heat sink was filled with PCM, here n-eicosane was used because of its high latent heat. All dimensions are in mm.

The setups are done the same as the validation [6.1]. The numerical study is done in two separate cases.

1. The numerical study on heat transfer from a PCM-based heat sink without baffles [6.3.1].
2. The is a numerical study on heat transfer from a PCM-based heat sink with baffles [6.3.3].

The computational domain without baffles is drawn as per the dimension.

6.3.1 Computational Domain of Heat Sink Without Baffles

The sketch is drawn as per the dimension mentioned in fig.6.3.17a. Extrude tool is used.

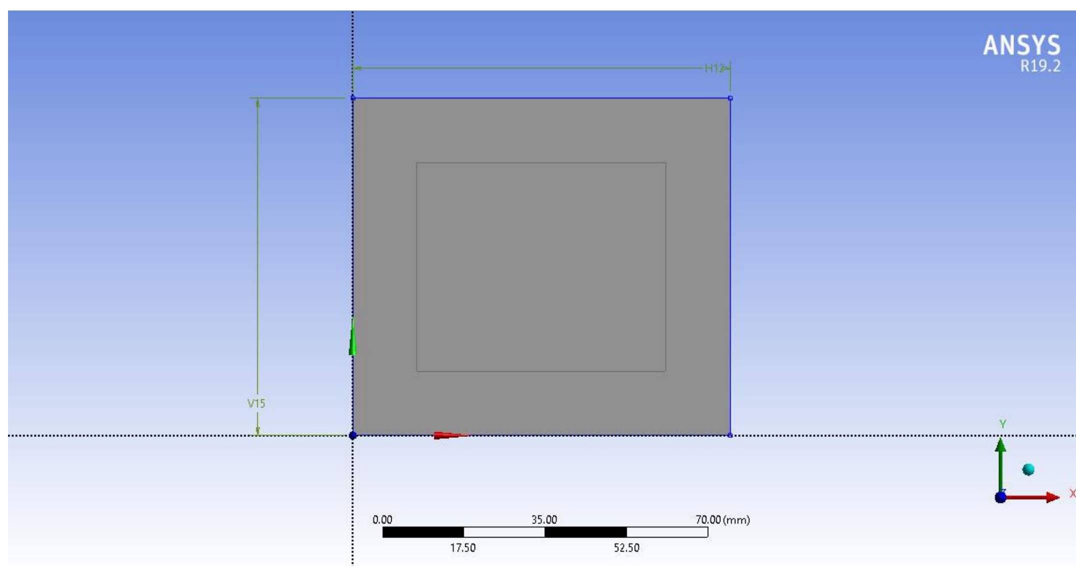

Fig. 6.3.18a

The body of the heat sink is made up of aluminium and inside the heat sink is filled with n-eicosane PCM. The properties of aluminium are given in the table (6.3.3.3).

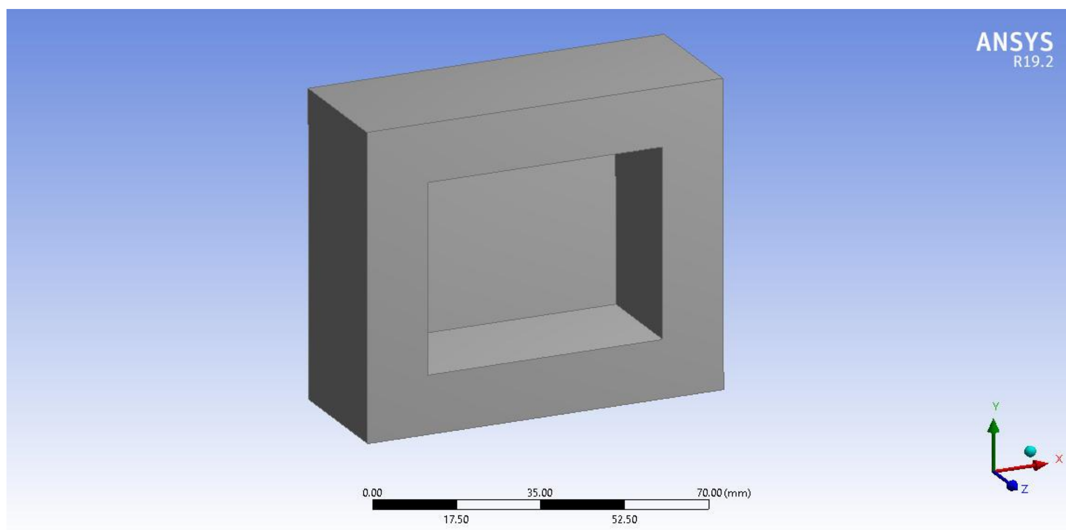

Fig.6.3.18b

Fig.6.3.18 a & b Computational domain of heat sink without baffles

Geometrical Details

- Base Size = 81.10*72.40mm
- Side wall thick = 30mm

6.3.2 Mesh Domain of Heat Sink Without Baffles

Grid independence study is performed for the heat sink configuration without baffles to decide on the number of mesh elements required for the numerical simulation. The heat sink configurations are tested for coarse, medium, and fine grids. For the heat sink configuration without baffles, the number of mesh elements considered is coarse, medium, and fine. A constant heat input of 851.55W/m^2 was applied at the bottom of the heat sink for 4000s.

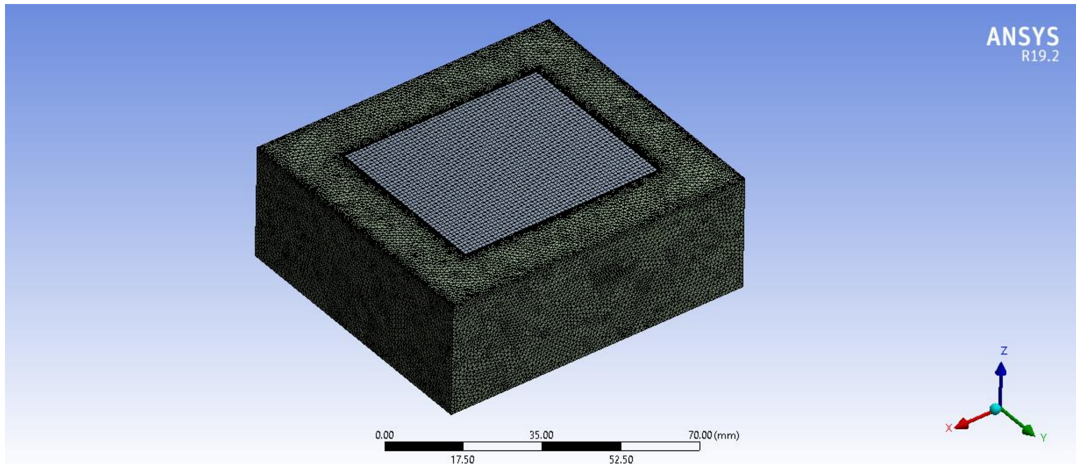

Fig.6.3.2.19 Meshing of heat sink without baffles

The numerical investigations are performed for a volumetric fraction of 0.9. The insulated boundary condition is applied to all the walls of the heat sink. The timestep value is 0.01s. The temperatures attained by the heater surface at different time instances for these mesh elements are plotted in Fig.6.3.2.20. From the results, it is evident that 613754 (fine mesh) mesh elements and the number of nodes 184729 are sufficient to carry out further numerical simulations.

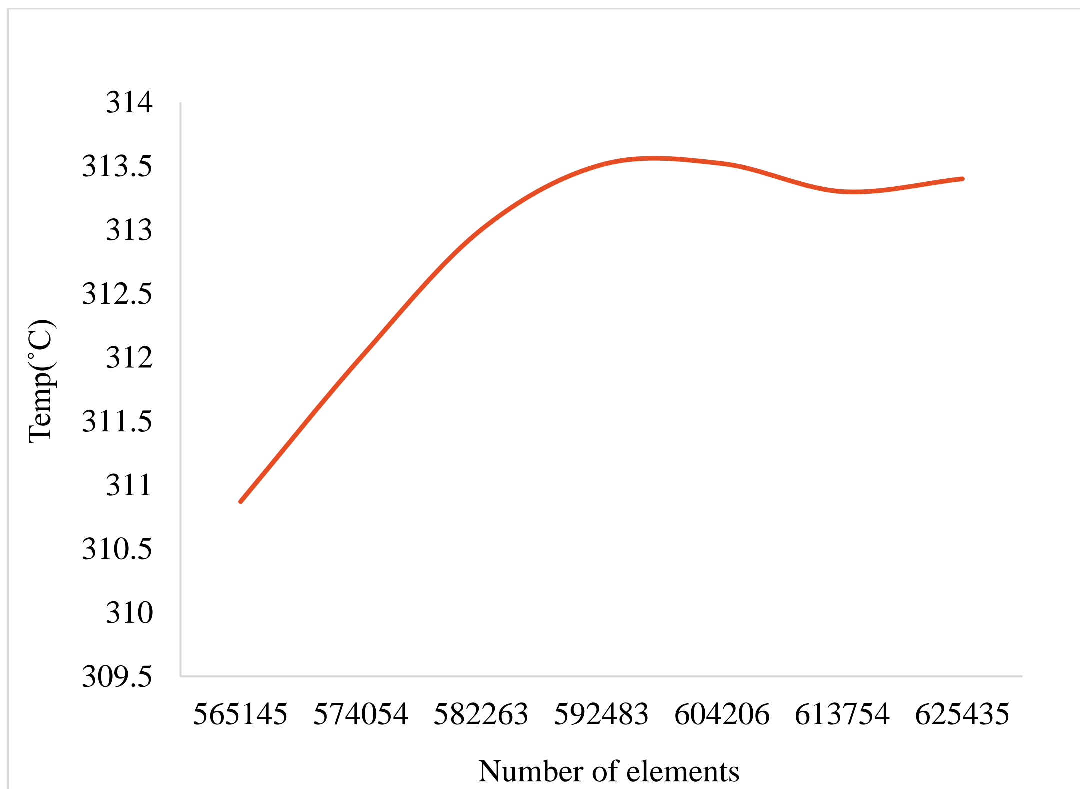

Fig.6.3.2.20 Grid independence study of heat sink without baffles

6.3.3 Computational Domain of Heat Sink with Baffles

The heat sink with baffles is drawn with the same dimensions used for without baffles. The dimension of baffle is height = 50.40mm, thickness = 3.90mm, and length = 35.80mm. Two baffles are demonstrated inside the heat sink. Fig.6.3.3.21a shows the front view of the geometry.

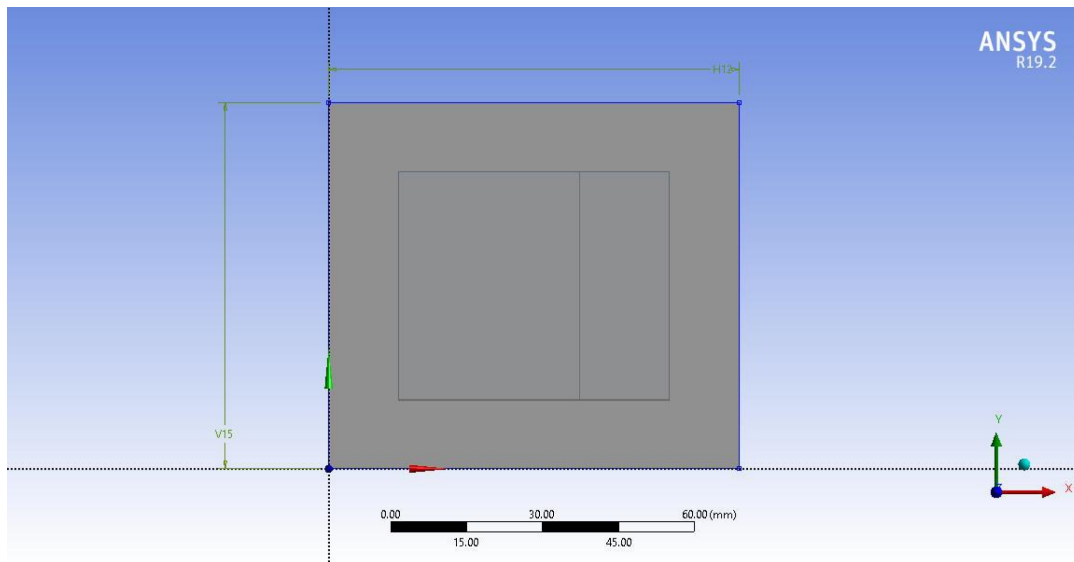

Fig.6.3.3.21a

It is drawn in design modeler by using extrude tool. Baffles are made up of aluminium (properties are given in table 6.3.3.3).

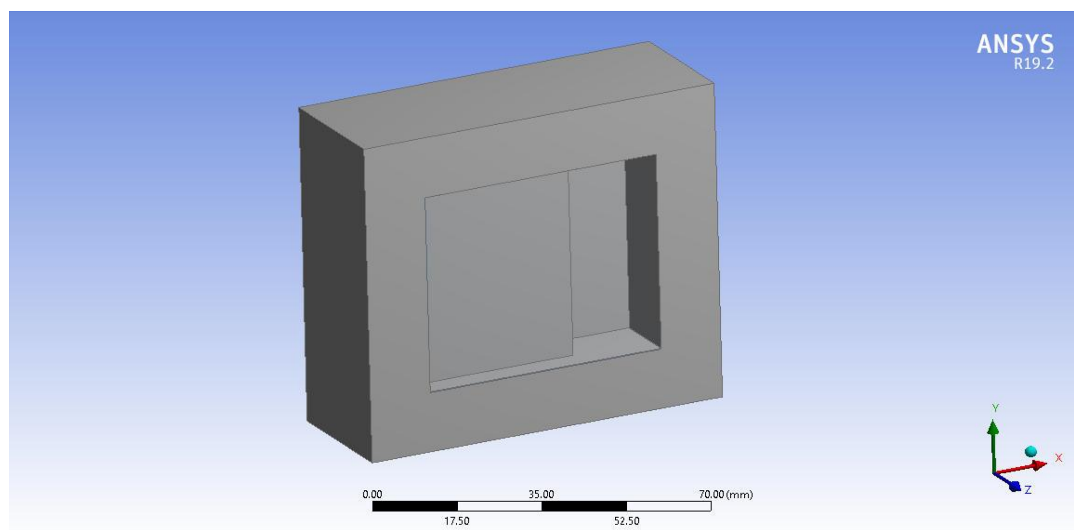

Fig.6.3.3.21b

Fig 6.3.3.21a & b Computational Domain of Heat Sink with Baffles

Table 6.3.3.3 Properties of Aluminium

Material	Thermal conductivity (W/mK)	Specific heat (kJ/kg)	Melting point (˚C)	Density (kg/m^3)
Aluminium	202.4	0.87	660.4	2719

6.3.4 Mesh Domain of Heat Sink with Baffles

For the heat sink arrangement without baffles, a grid independence study is conducted to determine the number of mesh elements needed for the numerical simulation. Coarse, medium and fine grids are used to test the heat sink layouts.

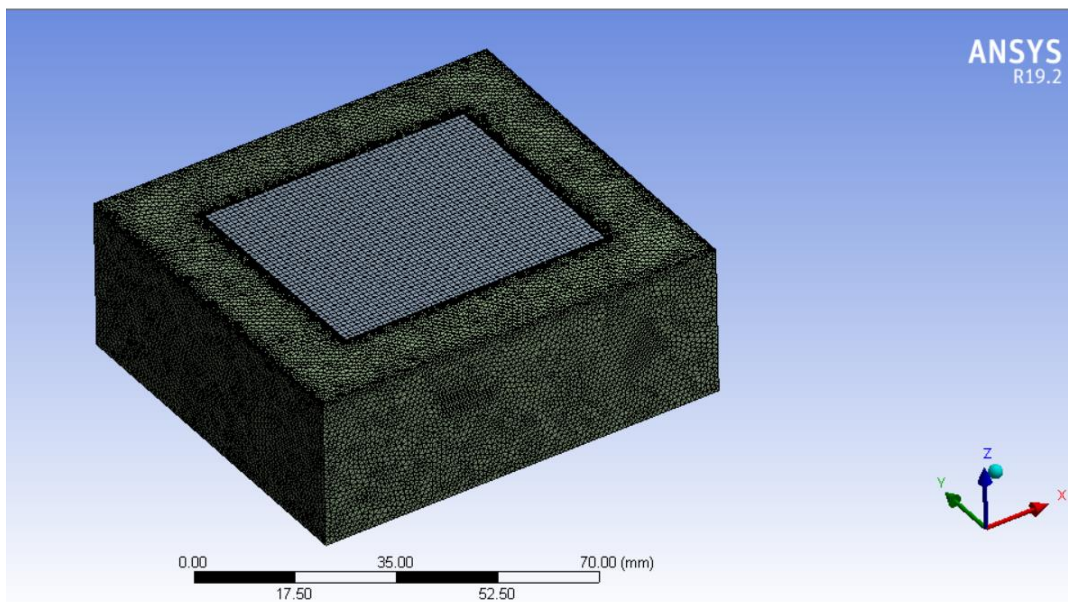

Fig.6.3.4.22 Meshing of the heat sink with baffles

The number of mesh elements taken into consideration for the heat sink layout without baffles is three: coarse, medium, and fine. At the base of the heat sink, a steady heat input of 851.55W/m^2 was applied for 4000s.

For a volumetric fraction of 0.9, numerical investigations are performed. The insulated boundary condition is applied to all the walls of the heat sink. The timestep value is 0.01sec. The temperatures attained by the heater surface at different time instances for these mesh elements are plotted in Fig.6.3.4.23. From

the results, it is evident that 711763 (fine mesh) mesh elements and the number of nodes 204180 are sufficient to carry out further numerical simulations.

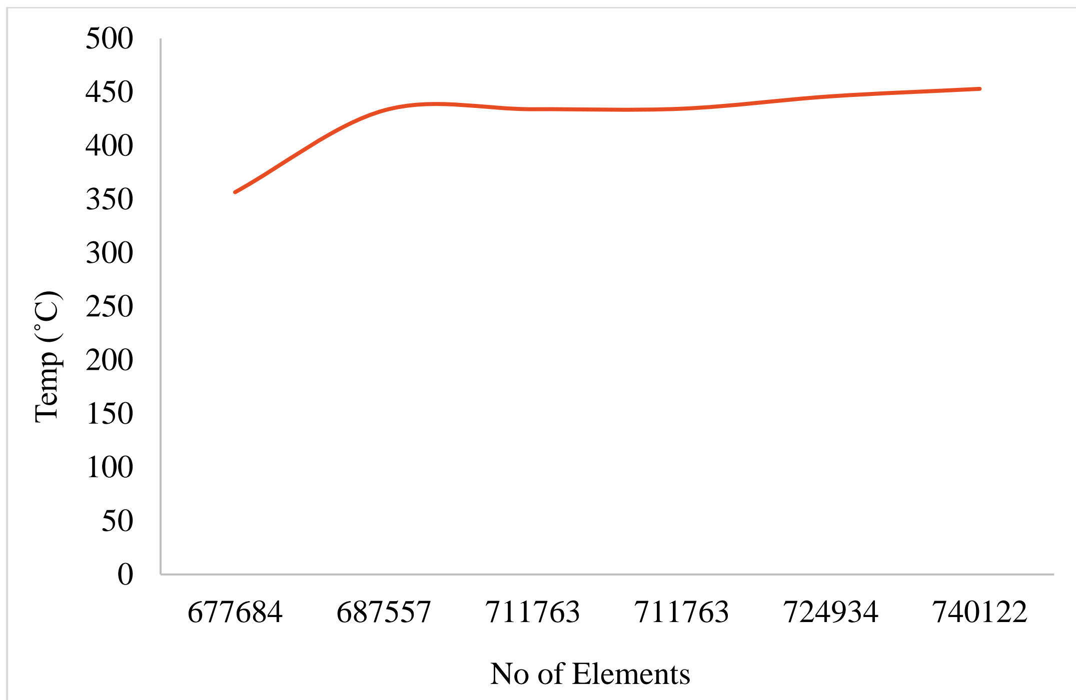

Fig.6.3.4.23 Grid independence study of the heat sink with baffles

6.3.5 Initial and Boundary Conditions

During charging and discharging cycles, the ambient circumstances are the same for both heat sink configurations - without and with baffles - but the performance of each heat sink varies. The existence of the PCM and its flow physics are the reasons. The aluminum and the PCM domains are initialized at 18°C. During the charging cycle, the heat input at the bottom surface is set at 851.55W/m^2. The side walls are considered adiabatic walls.

6.4 CONDUCT A COMPARATIVE STUDY BETWEEN N-EICOSANE & RUBITHERM PCM

This study aims to determine which of these two PCMs is more effective in both heat sinks with baffles and heat sinks without baffles. When we compare the properties of N-eicosane and Rubitherm, N-eicosane possesses high latent heat. This comparative study is done in two cases.

1. Heat sink without baffles was filled with PCMs i.e., n-eicosane & Rubitherm, and conducted a comparative study.
2. Heat sink with baffles was filled with PCMs and conducted a comparative study.

Table 6.4.4 Properties of Rubitherm

Name of PCM	Thermal Conductivity (W/mK)	Specific Heat (kJ/kg K)	Latent Heat (kJ/kg)	Melting Point (˚C)	Density (kg/m^3)
RT 42, Rubitherm	0.21 (both phases)	2	174	38-43	880 (solid) 760 (liquid)

CHAPTER 7

RESULTS AND DISCUSSION

7.1 NUMERICAL VALIDATION OF EXPERIMENTAL DATA

The results of the validation of experimental data are discussed in this section. The effect of heat sink configuration, effect of PCM amount, effect of heat flux and latent heat phase comparison of different heat configurations were plotted.

7.1.1 Effect of Heat Sinks Configurations

The following graph shows the effect of heat sink configuration on heat transfer. The dots represent the experimental values and curves represent the numerical values obtained from the simulation.

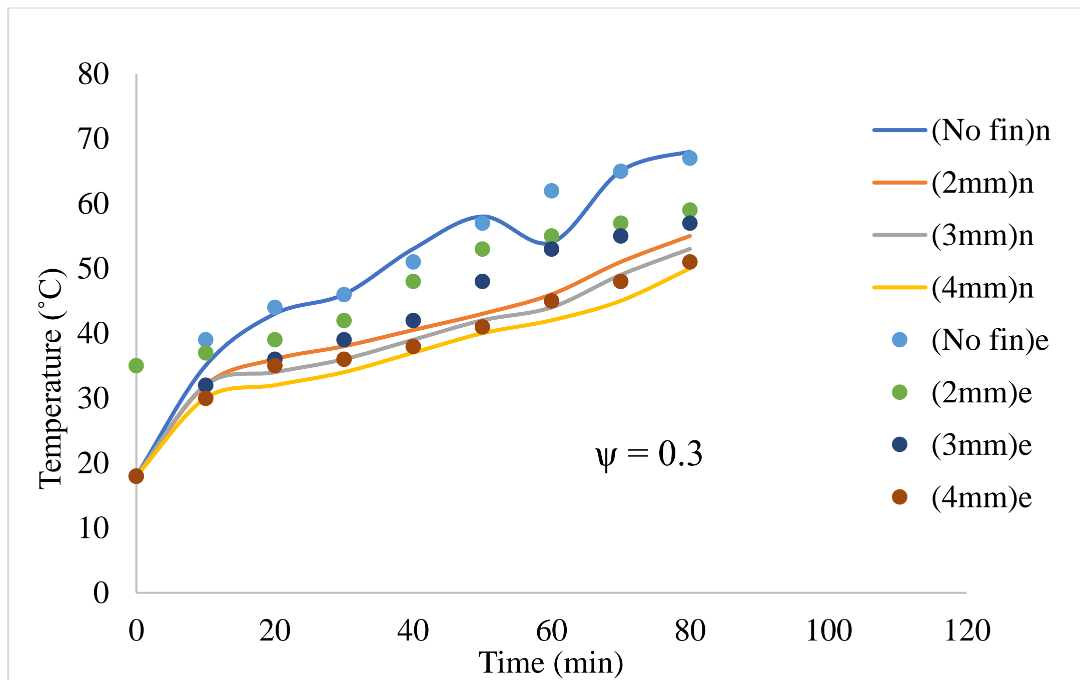

Fig. 7.1.1.24a Effect of fin thickness for $\psi = 0.3$ at 1.6 kW/m^2

The effect of fin thickness of each configuration of heat sinks is shown in Figs. 7.1.1.24a–7.1.1.24c. An input heat flux of 1.6 kW/m^2 for each volumetric fraction case of PCM was selected.

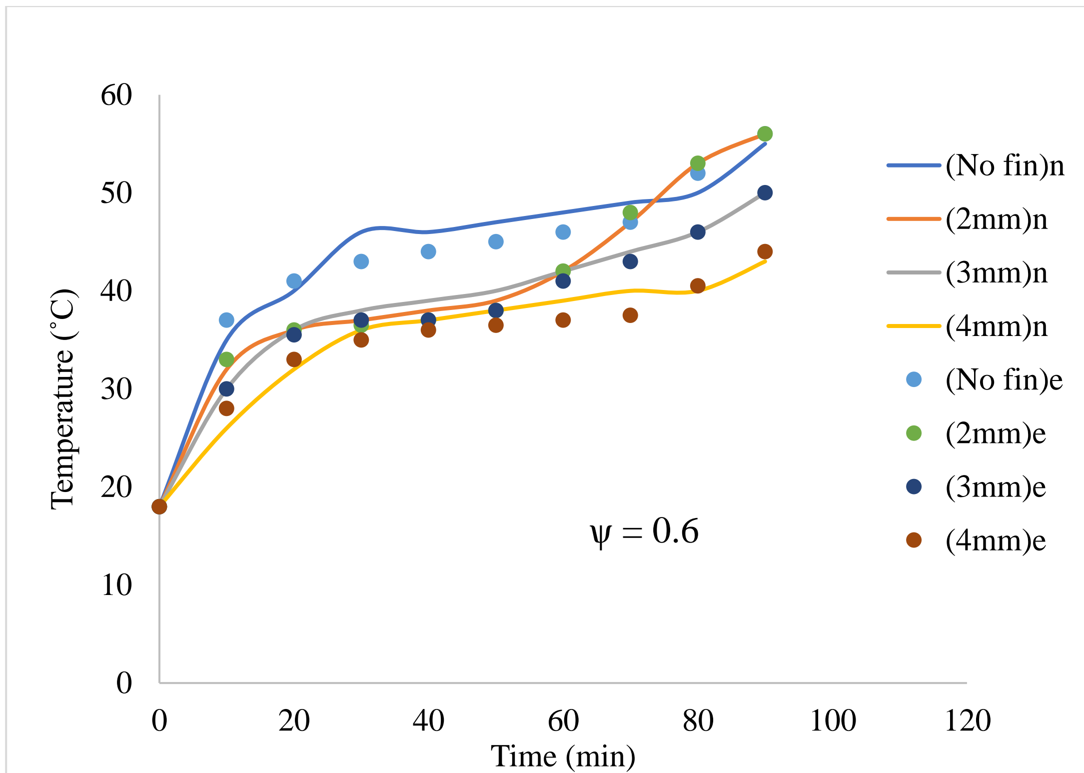

Fig.7.1.1.24b Effect of fin thickness for ψ = 0.6 at 1.6 kW/m^2.

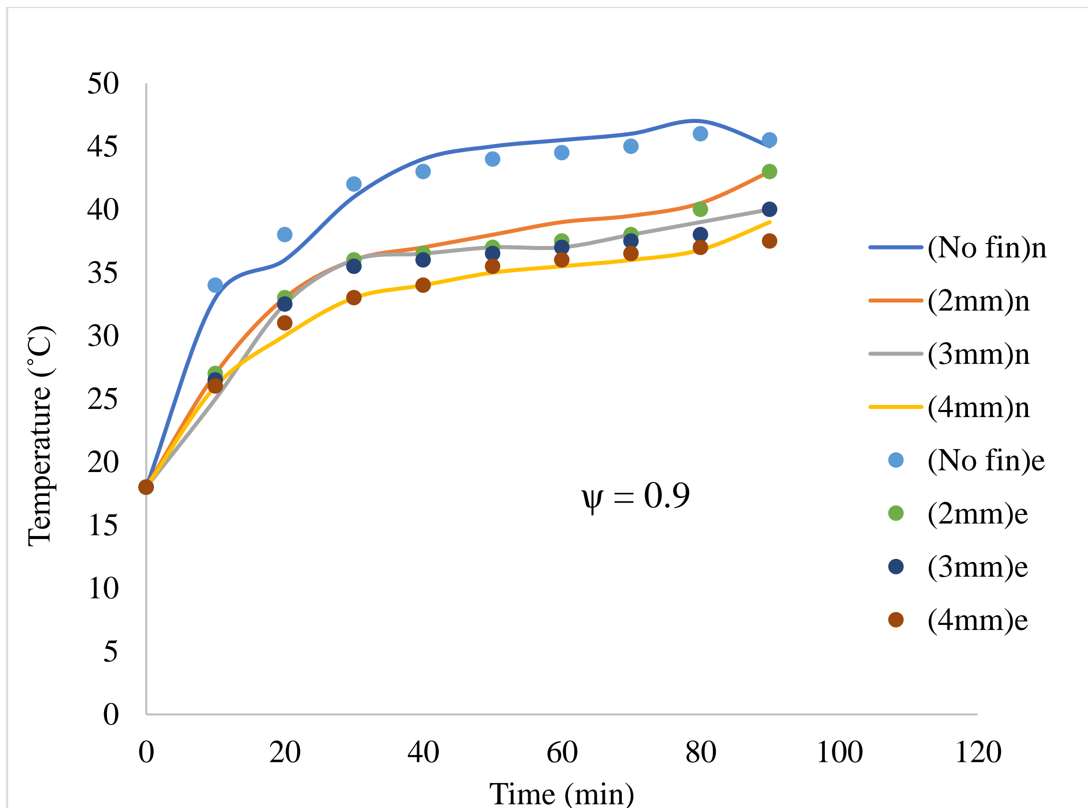

Fig.7.1.1.24c Effect of fin thickness for ψ = 0.9 at 1.6 kW/m^2

The optimum thermal performance for passive thermal management of electronic equipment is a heat sink filled with ψ = 0.9. As the maximum operating time for the case of ψ = 0.9 is reached, the device's base temperature is lowered and the operation duration is increased to a comfortable temperature limit. After 90 minutes of operation, a temperature of 38.5˚C (in numerical study) lower than the typical discomfort temperature is reached for a 3 mm thick fin case and the experimental value is 37.8˚C.

In all volumetric fraction graphs, a minor variance in temperature distribution is seen for pin-fin heat sinks that are 2 mm and 4 mm thick. At ψ = 0.3 and ψ = 0.6, the 2 mm fin thickness has a greater base temperature than the 4 mm fin thickness heat sink, which also achieves a higher temperature at ψ = 0.9. In the case of 2 mm thick fins, a higher number of fins may be to held responsible, and in the case of 4 mm thick fins, a larger pitch, as a higher number of fins and non-uniform distribution causes the rise of base temperature and results in local melting of PCM rather than distributed heat in PCM through fins.

7.1.2 Effect of PCM amount

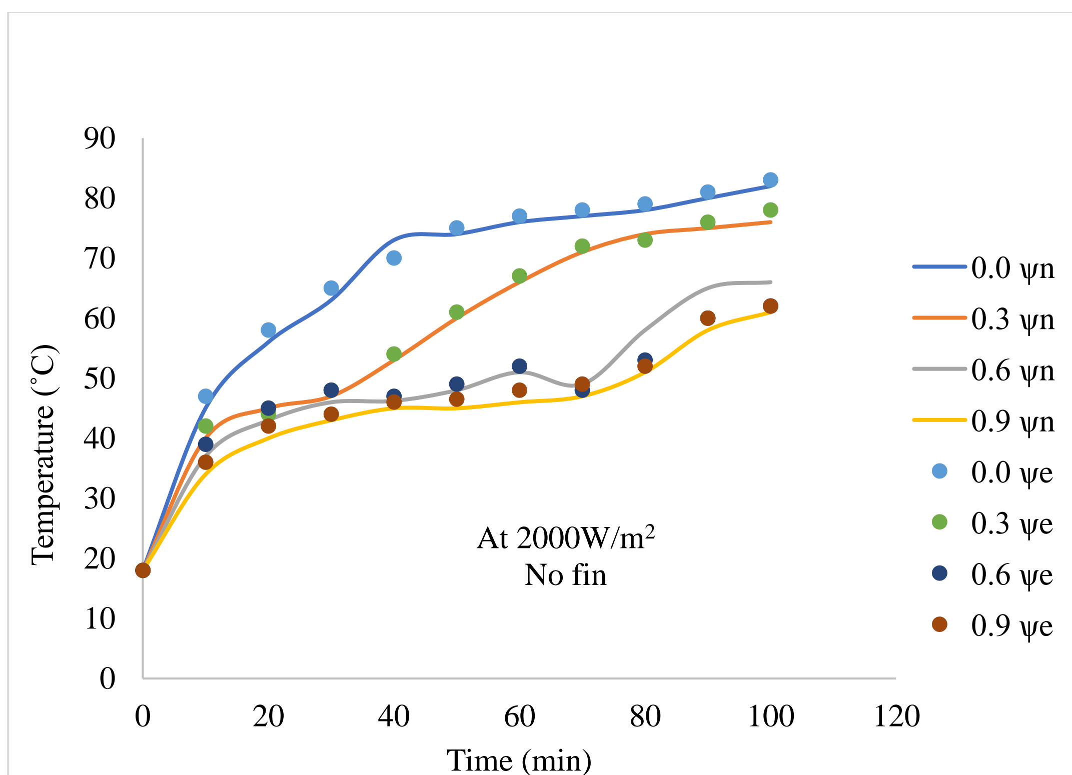

Fig.7.1.2.25 Time-temperature distribution for no fin heat sink at different ψ.

Four different percentage levels are chosen to determine the effect of PCM volume. Each configuration of the heat sink is filled with a volumetric ratio of (ψ 0.0, ψ 0.3, ψ 0.6, ψ 0.9) and an input heat flux of 2.0 kW/m^2 is provided for each case. Due to the absence of a PCM-filled heat sink, temperature increases quickly at ψ 0.0. Additionally, the thermal performance of the heat sink is significantly impacted by the elongation of the latent heat phase for pin-fin heat sink configurations when the heat sink is filled for three equal fractions of PCM. This demonstrates the important role that a heat sink with a volumetric fraction of ψ 0.9 plays in the thermal control of electrical devices.

7.1.3 Effect of heat flux

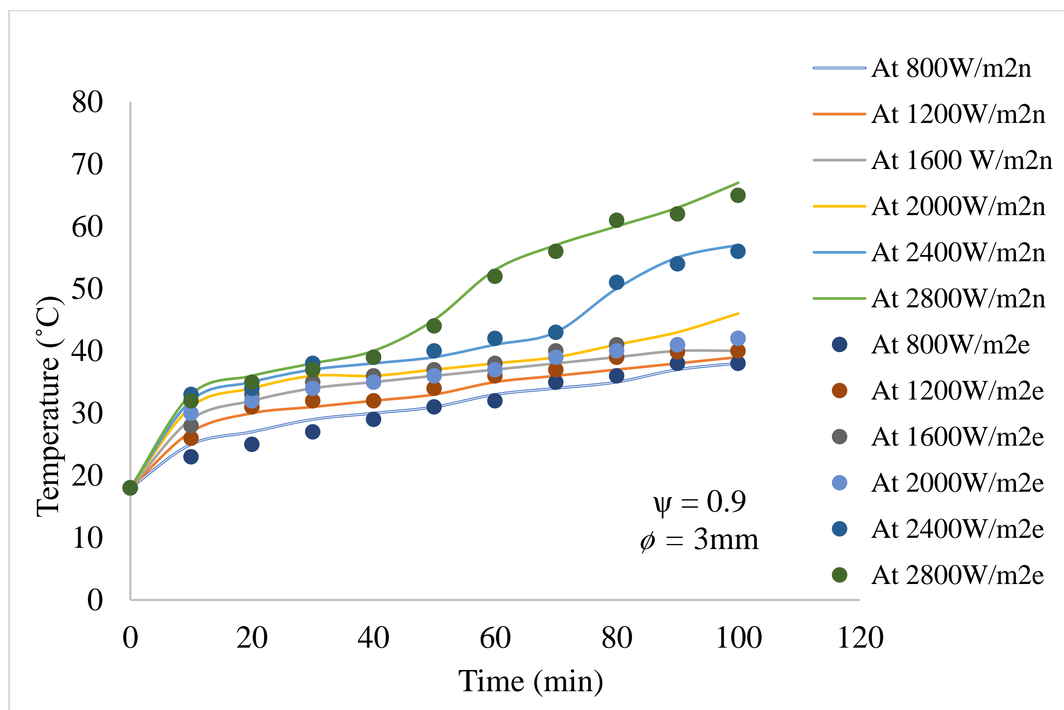

Fig.7.1.3.26 Phase change variations at different input heat fluxes for 3 mm thick pin-fin heat sink.

For a 3 mm thick pin-fin heat sink filled at ψ = 0.9 of PCM (n-eicosane), the heat fluxes between 0.8 and 2.8 kW/m^2 with a step of 0.4 kW/m^2 were chosen to reflect the effects of the various heat fluxes. As the input heat density rate rises, it can be seen that the latent heat phase change slows down. The PCM does not undergo a phase shift even after 100 minutes of heating, and heat is absorbed inside the PCM because of its high latent heat capacity, according to a careful observation of heat flux rates of 0.8 kW/m^2 and 1.2 kW/m^2. For a heat flux of 2.8 kW/m^2, on

the other hand, the temperature rises quickly after the latent heat phase has been heating for just around 40 minutes. Pre-melting and post-melting sensible heating are the names of the phases that come before and after the latent heat phase. For the passive phase change cooling of electrical devices, these phases are less significant. As the temperature increases quickly, electronics base temperature remains at a comfortable level.

Table 7.1.3.5 Enhancement in time to reach 40˚C, 3mm thickness pin fin heat sink,

Heat flux W/m^2	Time (min)		
	Experimental study (Arshad, et al. (2018)	Numerical study	% Difference
2000	77.25	75	2.9
2400	55.25	50	9.5
2800	42	41	2.38

7.1.4 Latent heat phase comparison

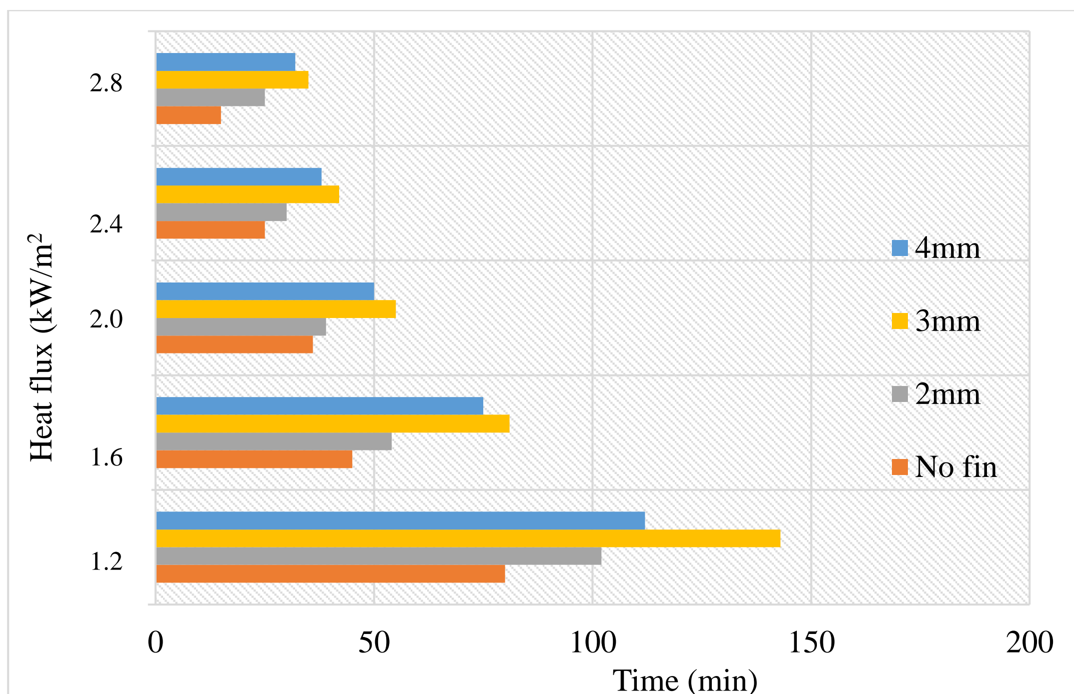

Fig.7.1.4.27 Latent heating phase completion durations for different configuration heat sinks.

By comparing the completion times of the latent heat phase, it is possible to determine the thermal performance of pin-fin heat sinks affected by PCM. The crucial region for passive cooling of electrical devices employing finned heat sinks built on PCMs is the latent heat phase. Given this, the Fig7.1.4.27 compares four heat sinks with various layouts at input heat fluxes of 1.2 to 2.8 kW/m^2. The highest latent heat phase completion time in comparison to the other heat sinks can be seen in a clear image of a 3 mm thick pin-fin heat sink.

When the input heat density is 1.2 kW/m^2, the maximum time gained is 140 minutes, however when the heat input density is 2.8 kW/m^2, the maximum time gained is 36 minutes for a heat sink with a 3 mm fin thickness is obtained in experiment; whereas in numerical it is 142 minutes and 37 minutes respectively. The fact that the phase reduced as the rate of delivered heat flux increased is another indication of heat flux with a latent heating phase. The ideal fin configuration of a 3 mm pin-fin heat sink with increased surface area transfers heat through the PCM more effectively. Therefore, a pin-fin heat sink made of a material with a higher thermal conductivity can be used to make up for the PCM's lower thermal conductivity. This increases the rate at which heat is transferred, which enhances the thermal performance of electronic devices.

7.2 NUMERICAL STUDY OF HEAT SINK WITH BAFFLES AND WITHOUT BAFFLES

The temperature-time graph can be plotted in ANSYS Fluent. From this, we can understand the variation of the charging period. Here N-eicosane is used as PCM.

7.2.1 Variation of charging period in PCM-based heat sink without baffles

Variations in temperature with time can be seen. Area weighted average of total temperature is on Y-axis, and flow time is on the X-axis. The average temperature of both heat sink and PCM represents the area-weighted average of total temperature. The period of time it takes for PCM to change phases is known as the flow time. The initial temperature of the PCM-based heat sink is 18˚C. when flow time increases temperature also increases. This graph represents the charging period of PCM.

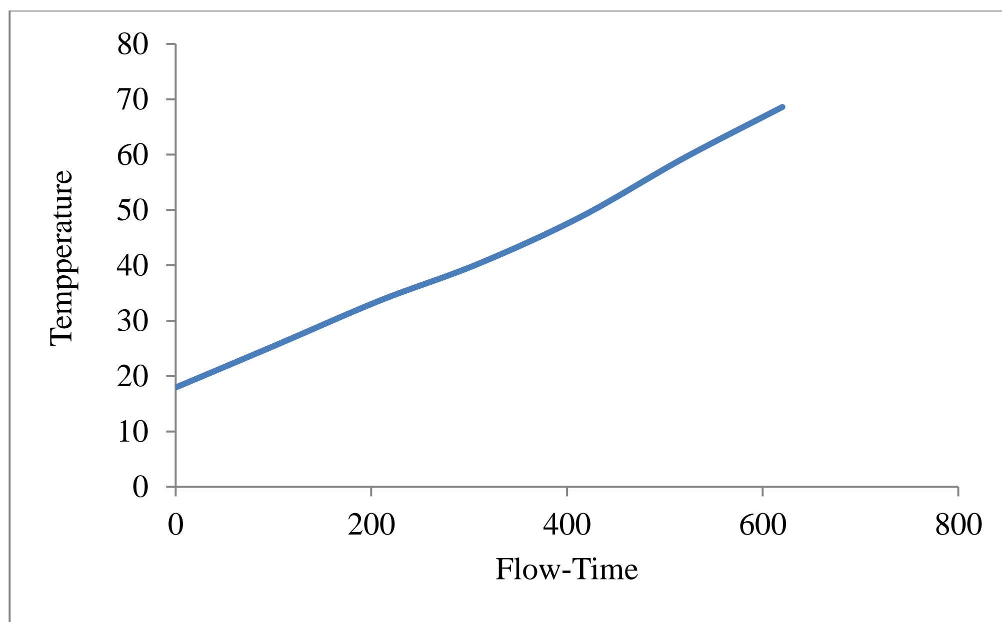

Fig.7.2.1.28 Temperature-time graph (heat sink without baffles)

7.2.2 Variation of liquid-fraction of PCM in without baffles

The variation of the liquid fraction with time is given in fig.7.2.2.29 From this, we can say that after 100 min, PCM starts to melt and at 450 min it becomes fully liquid.

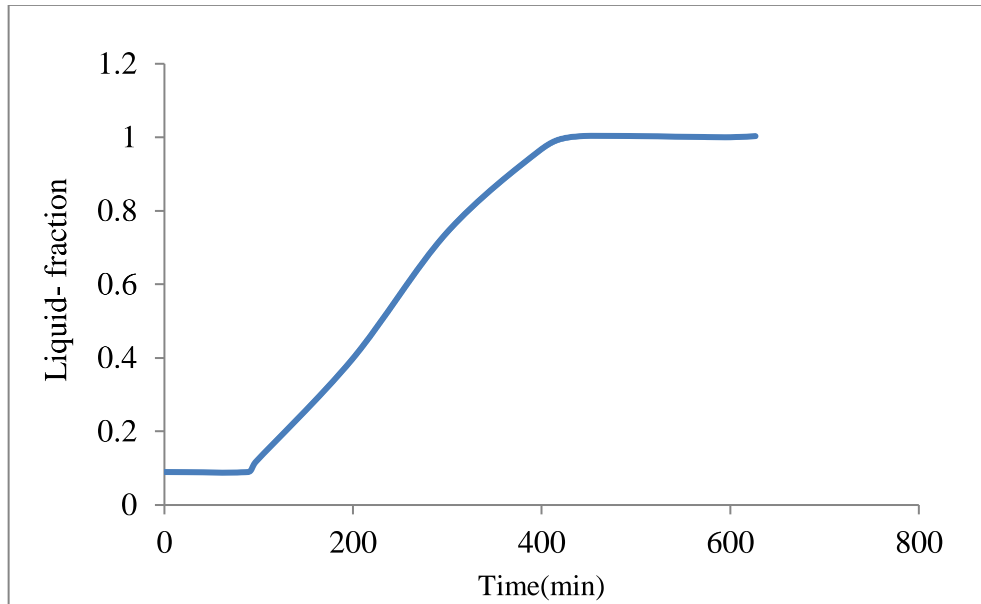

Fig.7.2.2.29 Liquid fraction – time graph (heat sink without baffles)

In this case (PCM-based heat sink without baffles), thermal conductivity is very low, so heat transfer takes time.

7.2.3 Variation of Charging period in PCM-based heat sink with baffles

The initial temperature is the same as that of the heat sink without baffles. The temperature increases with time, but it is different from the graph of heat sink without baffles. Here we use baffles, which enhance the heat transfer rate of the heat sink.

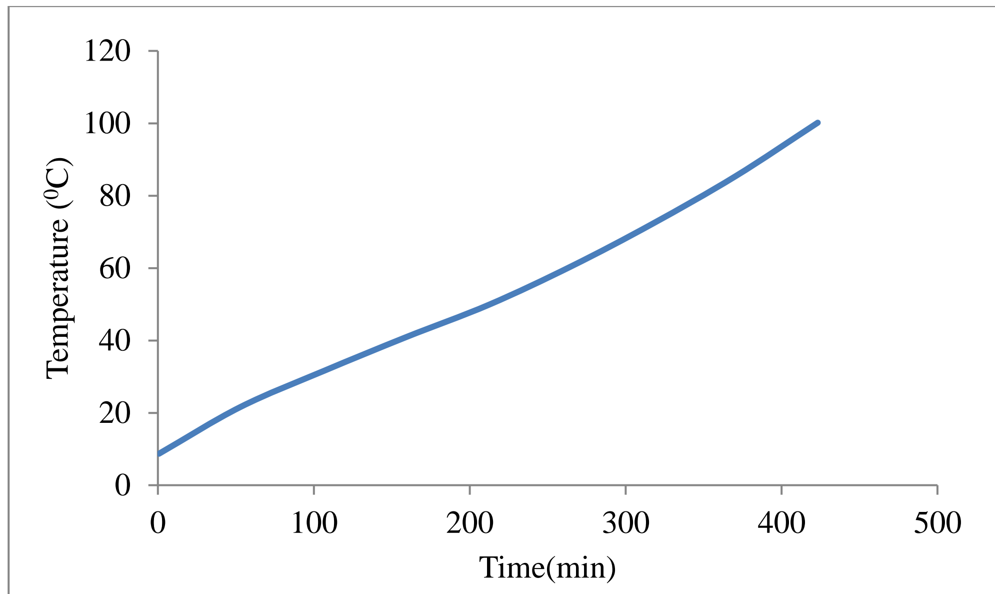

Fig.7.2.3.30 Temperature-time graph (heat sink with baffles)

7.2.4 Variation of liquid-fraction of PCM in with baffles

Variation of the liquid fraction with time is plotted in the graph fig. From this, we can say that the melting of PCM starts after 30min and it becomes fully liquid at 350min.

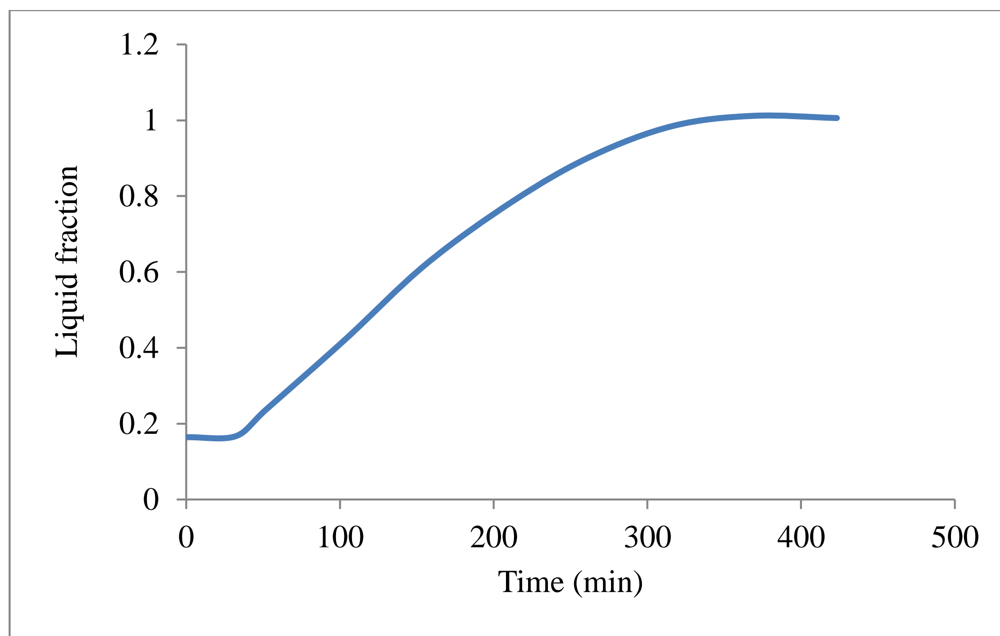

Fig.7.2.4.31 Liquid fraction-time graph (heat sink with baffles)

7.2.5 Temperature comparison between with and without baffles

Temperature variation with baffles shows a rapid increase compared to without baffles. This is because of the presence of TCEs, which increase the thermal conductivity, surface area, and heat transfer. The heat sink without baffles gives a temp of 50˚C at 450 min., whereas the heat sink with baffles gives 103˚C. It has been concluded that the charging time of PCM can be increased by using baffles inside the heat sink.

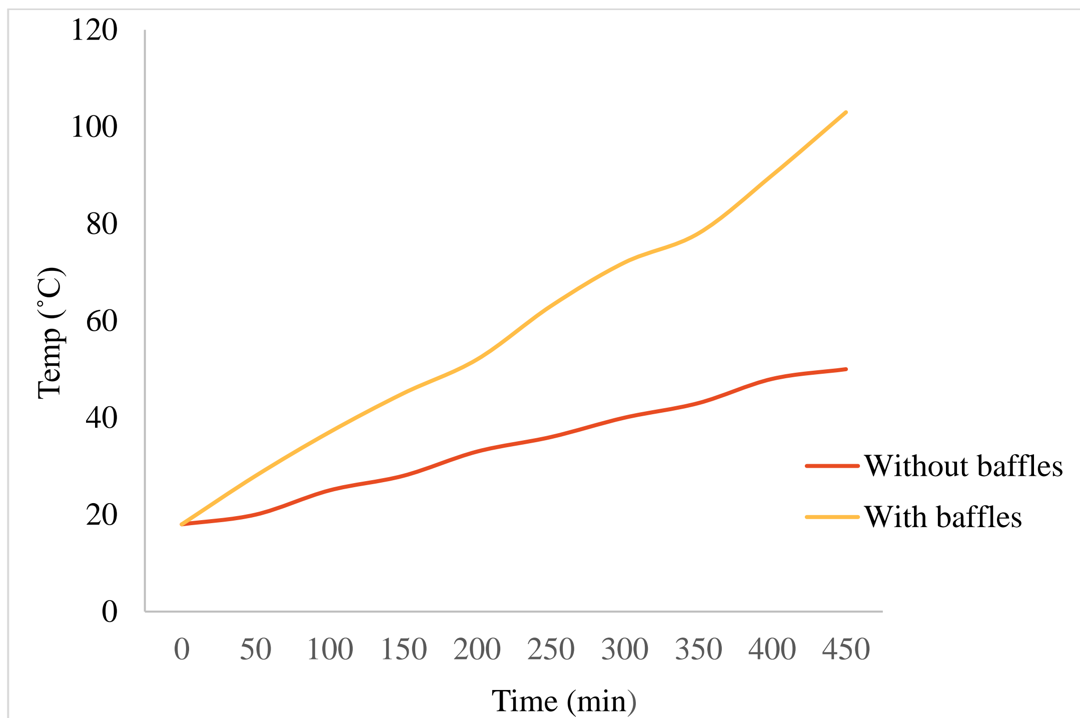

Fig.7.2.5.32 Temperature comparison

Table 7.2.5.6 Comparison of temperature

Time (min.)	Temperature (˚C)	
	Without baffles	With baffles
450	50	103

7.2.6 Liquid fraction comparison between with and without baffles

Melting begins in a PCM in a heat sink with baffles after a few minutes, whereas it takes 100 minutes in a PCM without baffles for melting to begin. PCM inside the with-baffles liquefies first, i.e., at 350 minutes, PCM becomes completely liquid. But without baffles, it takes 450 min. to reach the liquid fraction of 1. The difference between the two conditions, with and without baffles, is 100 minutes. When the heat transfer rate increases, PCM takes heat and reaches its melting temperature.

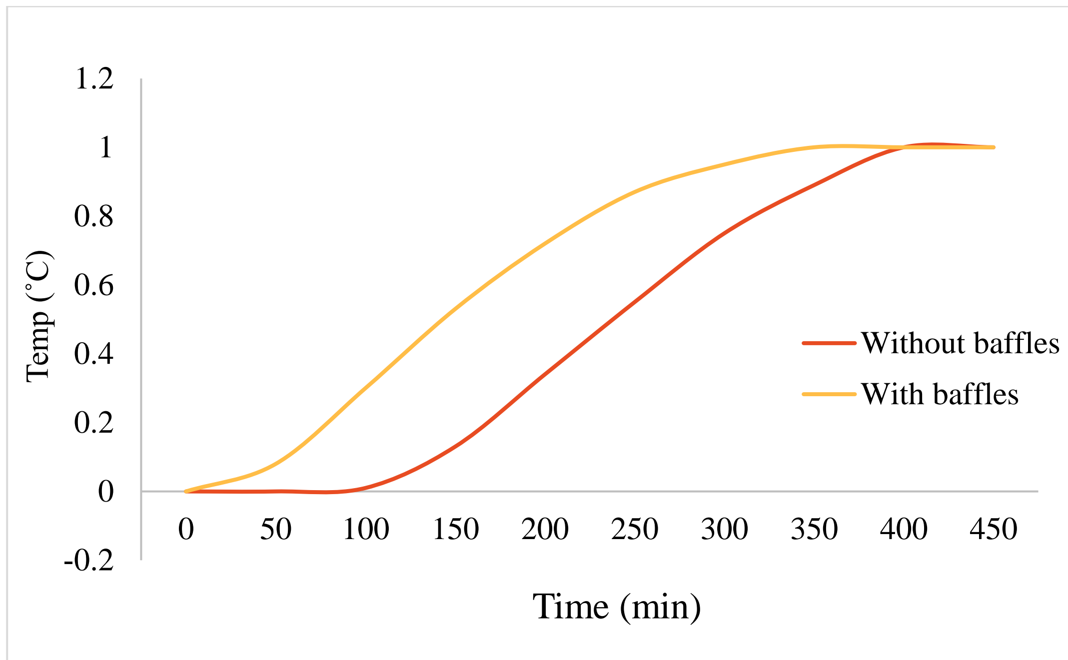

Fig.7.2.6.33 Liquid fraction comparison

Table 7.2.6.7 Comparison of the liquid fraction

Liquid fraction	Time (min.)	
	Without baffles	With baffles
1	450	350

From fig.7.2.5.32, it shows heat transfer in with baffles is high compared to without. TCE plays an important role in heat transfer.

7.3 COMPARATIVE STUDY BETWEEN N-EICOSANE & RUBITHERM PCM

A comparative study of N-eicosane and Rubitherm is done. From this investigation, it can be noted that these two PCMs have different charging periods. This comparative study can be divided into two cases;

1. PCM-based heat sink without baffles
    - Numerical simulation with rubitherm
    - Numerical simulation with n-eicosane (7.2.1)
2. PCM-based heat sink with baffles
    - Numerical simulation with rubitherm
    - Numerical simulation with n-eicosane (7.2.3)

7.3.1 Variation of Charging period in PCM-based heat sink without baffles (Rubitherm)

The initial temperature was 18˚C, from which its temperature was going to rise.

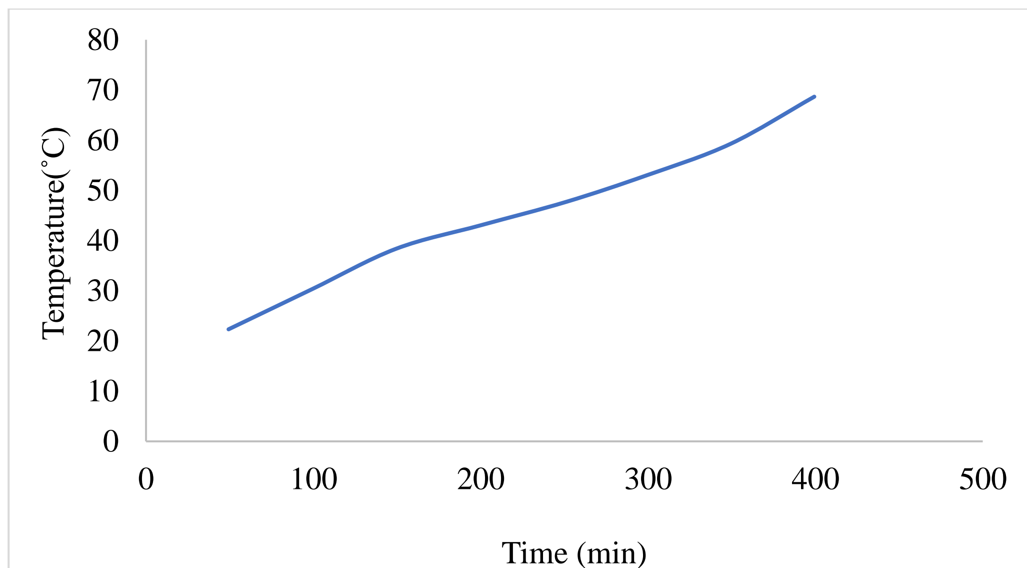

Fig. 7.3.1.34 Temperature-time graph of Rubitherm (without baffles)

7.3.2 Variation of The Liquid Fraction of Rubitherm

The melting of Rubitherm starts after 130 minutes. At 130 min. the temperature is 39˚C. That is, the melting temperature of Rubitherm is 38˚C. When the melting point increases, it takes more time to reach that temperature.

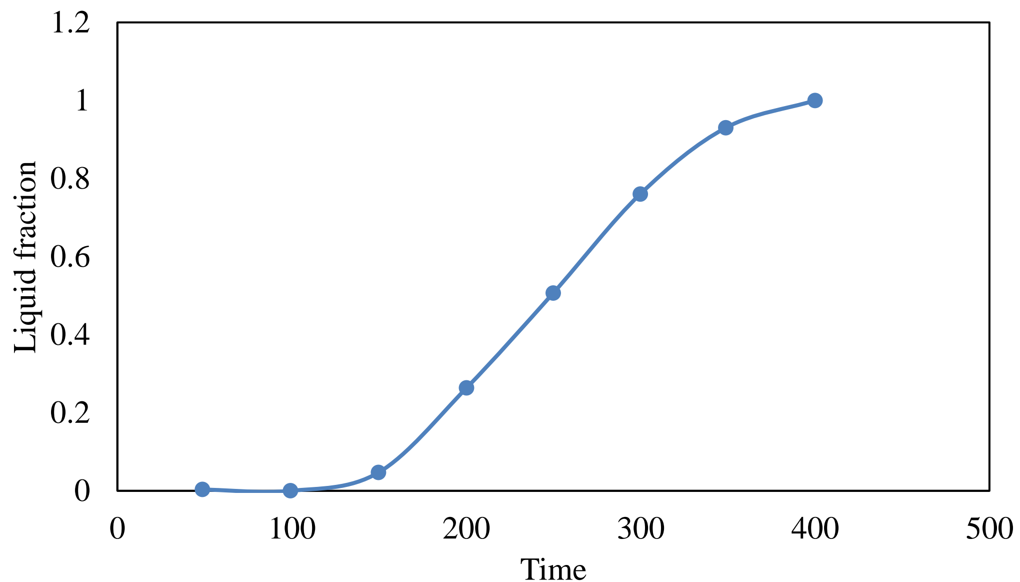

Fig.7.3.2.35 Liquid fraction of Rubitherm (without baffles)

7.3.3 PCM-based heat sink without baffles (Temperature)

When the temperature of Rubitherm and n-eicosane are plotted simultaneously. At 440 min, it is observed that the temperature of Rubitherm is greater compared to that of n-eicosane. At 440 min Rubitherm temp is 70˚C and n-eicosane temp is 50˚C. That means the thermal conductivity of Rubitherm is higher than that of n-eicosane.

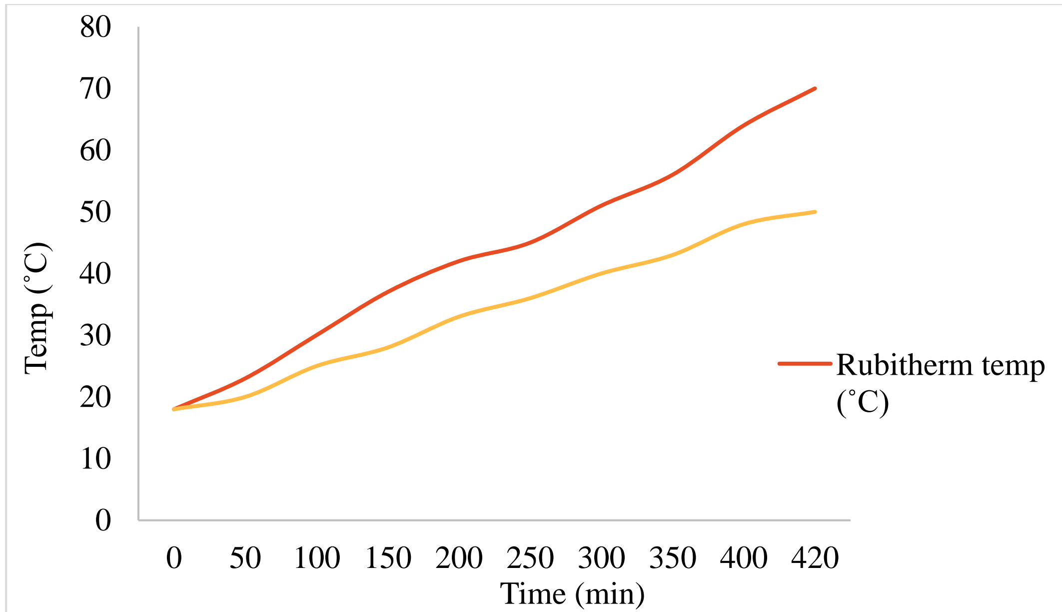

Fig.7.3.3.36 Comparison between rubitherm temperature and n-eicosane temperature (without baffles)

Table 7.3.3.8 Temperature comparison between rubitherm and n-eicosane (without baffles)

Time (min)	Temperature (˚C)	
	Rubitherm	N-eicosane
440	70	50

7.3.4 PCM-based heat sink without baffles (Liquid fraction)

N-eicosane starts to melt first because of its low melting point. But it takes time to completely liquefy. Rubitherm starts to melt after 150 minutes; it completely liquefies at 400 minutes. Rubitherm melts faster than n-eicosane.

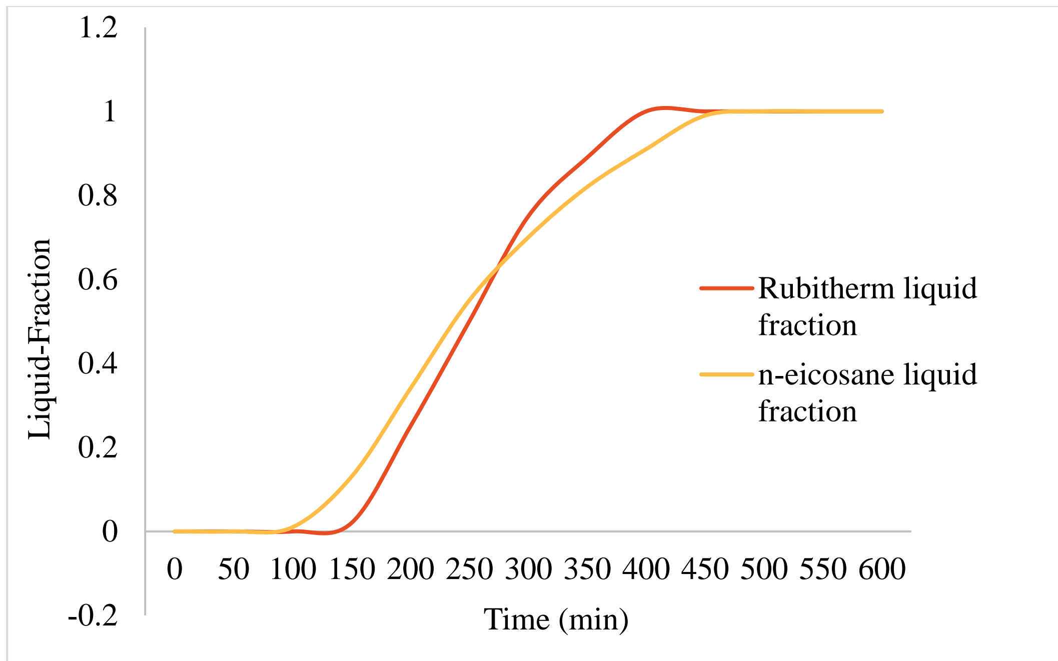

Fig.7.3.4.37 Comparison of the liquid fraction of rubitherm and n-eicosane (without baffles)

Table 7.3.4.9 Liquid fraction comparison between rubitherm & n-eicosane (without baffles)

Liquid fraction	Time (min)	
	Rubitherm	N-eicosane
1	400	500

7.3.5 Variation of Charging period in PCM-based heat sink with baffles (Rubitherm)

Compared to without baffles, with baffles shows some increase in temperature. This is because of the presence of baffles; these act as a TCE.

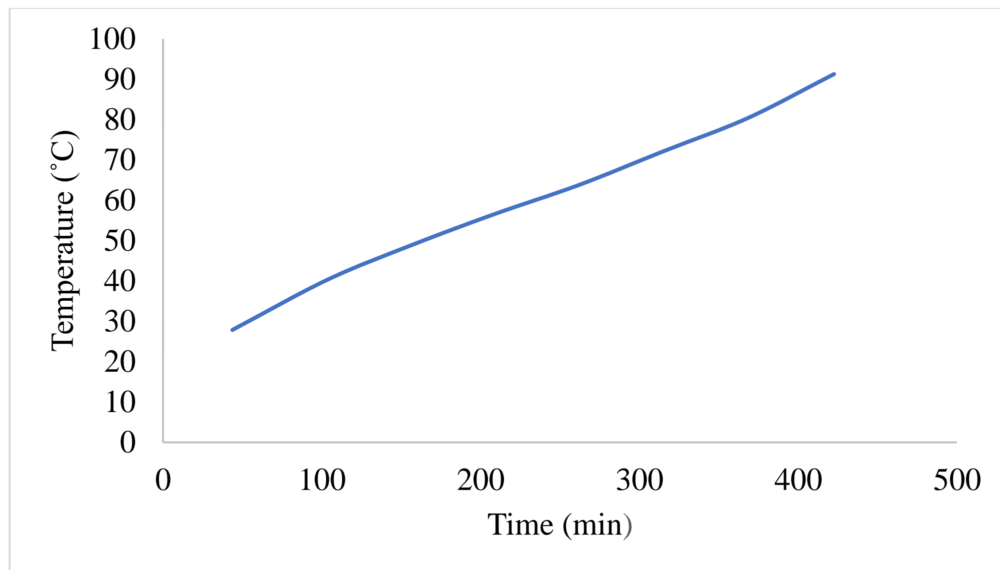

7.3.5.38 Temperature-time graph of Rubitherm (with baffles)

7.3.6 Variation of The Liquid Fraction of Rubitherm (with baffles)

Melting of rubitherm begins after 100 minutes and it becomes fully liquid after 375 minutes.

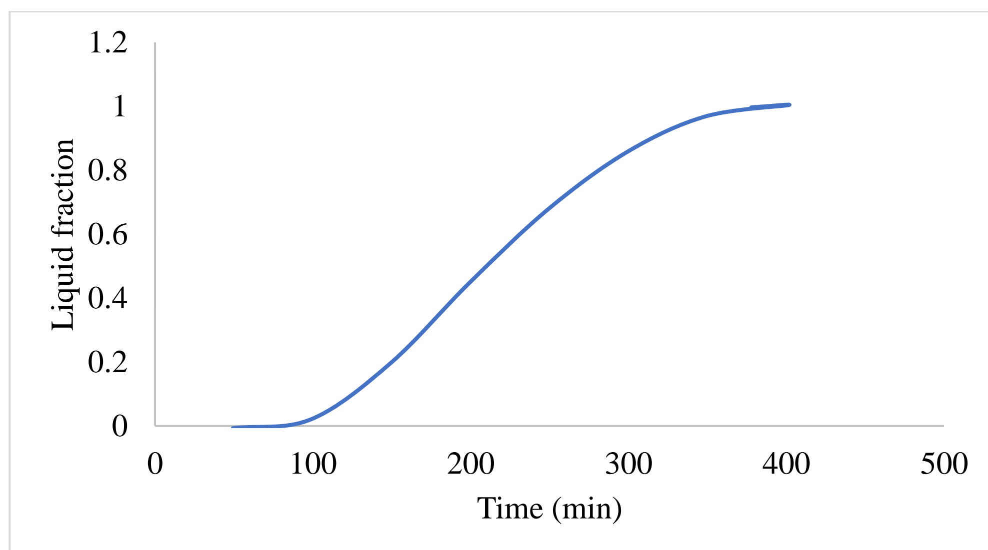

Fig.7.3.6.39 Liquid fraction of rubitherm (with baffles)

7.3.7 PCM-based heat sink with baffles (Temperature)

In the case of with baffles, n-eicosane shows high temp. at 400min, the temp is 99˚C. Whereas Rubitherm temp is 90˚C.

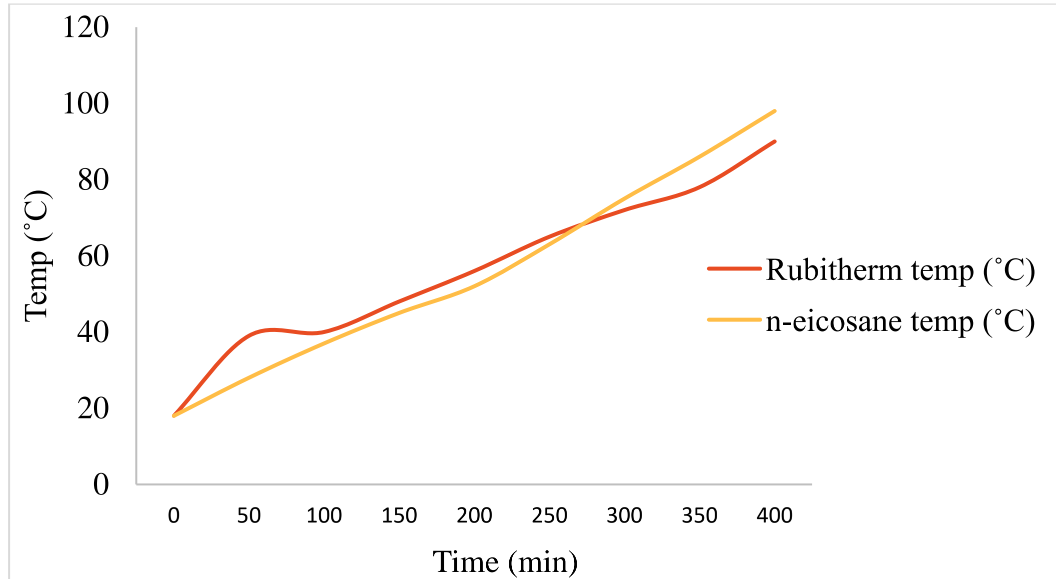

Fig.7.3.7.40 Comparison between rubitherm temperature and n-eicosane temperature (with baffles)

Table 7.3.7.10 Temperature comparison between rubitherm and n-eicosane (with baffles).

Time (min)	Temperature (˚C)	
	Rubitherm	N-eicosane
400	90	99

7.3.8 PCM-based heat sink with baffles (Liquid fraction)

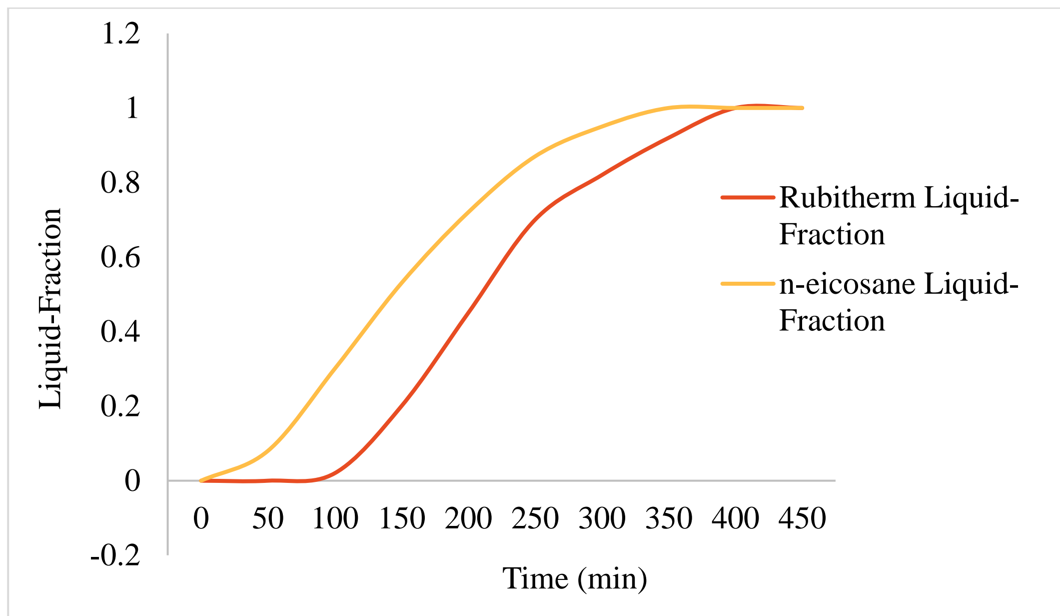

Fig.7.3.8.41 Comparison of the liquid fraction of rubitherm and n-eicosane (with baffles)

N-eicosane liquifies completely at 350 min whereas Rubitherm liquifies at 400min.

Table 7.3.8.11 Liquid fraction comparison between rubitherm and n-eicosane (with baffles)

Liquid fraction	Time (min)	
	Rubitherm	N-eicosane
1	400	350

CHAPTER 8

CONCLUSION

Four different volumetric fractions with heat flux range of 0.8-2.8Kw/m^2 (provided to different configurations of pin fin heat sink geometry to determine the thermal efficiency) were validated (Arshad, H.M. and Ali, et al. (2018). The conclusions are given below,

- The influence of the PCM with the heat sink increases the maximum operation time while lowering the temperature at ψ 0.9.
- By reducing the temperature, a 3 mm thick pin-fin heat sink filled with different volumetric fractions assures the elongation in the latent heating phase. (Fig. 7.1.4.27)
- For a pin-fin heat sink with 3 mm thick fins, the longest latent heating phase completion times were reported (in numerical) to be 58 min and 37.5 min for 2.0 kW/m^2 and 2.8 kW/m^2, respectively. And in experiment, the values are 59 min and 38 min respectively.
- When 2000W/m^2, 2400W/m^2, and 2800W/m^2 were provided in a 3mm thick pin fin, there was a 2.9%, 9.2%, and 2.38% difference was obtained between experimental and numerical values.

A numerical investigation on heat transfer from a PCM based heat sink with and without baffles was conducted to study the effectiveness of heat sink due to the presence of baffles and it is observed that heat sink with baffles can transfer more heat when compared to without baffle case. Also, a comparative study was conducted to determine which PCM gives the good performance. From numerical analysis the following results were obtained;

- More than 51% of increase in charging period were obtained in PCM based heat sink with baffles.
- Comparing N-eicosane and Rubitherm, n-eicosane shows good performance in heat sink with baffles and Rubitherm shows good performance in heat sink without baffles.

REFERENCES

A. Arshad et al., (**2017**) Thermal performance of phase change material (PCM) based pin-finned heat sinks for electronics devices: effect of pin thickness and PCM volume fraction, *Appl. Therm. Eng*. 112 143–155.

Ali Elghool and Firdaus Basrawi et al. (**2017**) A review on heat sink for thermo-electric power generation: Classifications and parameters affecting performance, *Energy Conversion and Management* 134,260–277.

ANSYS Fluent software package: user’s manual R19.2, (**2019**).

Arshad, H.M. and Ali, et al. (**2018**) experimental study of enhanced heat sinks for thermal management using n-eicosane as phase change material, *Application of Thermal Engineering* 52-66.

Baby R and C. Balaji, (**2012**) Thermal management of electronics using phase change material-based pin fin heat sinks, in 6th European Thermal Sciences Conference, *Journal of Physics*, IOP Publishing.

Baby R. and C. Balaji, (**2013**) Thermal optimization of PCM based pin fin heat sinks: an experimental study, *Application of Thermal Engineering* 54 (1) 65–77.

F.L. Tan and C.P. Tso, (**2004**) Cooling of mobile electronic devices using phase change materials, *Application of Thermal Engineering* 24 (2–3) 159–169.

G. Setoh, F.L. Tan, et al. (**2010**) Experimental studies on the use of a phase change material for cooling mobile phones, *Application of Thermal Engineering* 37 (9) 1403–1410.

Gharbi S., S. Harmand, et al. (**2015**) Experimental comparison between different configurations of PCM based heat sinks for cooling electronic components, *Application of Thermal Engineering* 87 454–462.

K.C. Nayak et al., (**2006**) A numerical model for heat sinks with phase change materials and thermal conductivity enhancers, *Int. J. Heat Mass Transf.* 49 (11–12) 1833–1844.

R. Kandasamy, X.-Q. Wang, et al. (**2008**) Transient cooling of electronics using phase change material (PCM)-based heat sinks, *Application of Thermal Engineering* 28 (8) (2008) 1047–1057.

R. Pakrouh et al., (**2015**) A numerical method for PCM-based pin fin heat sinks optimization, *Energy Convers. Manage*. 103 542–552.

R. Pakrouh, M.J. Hosseini, A.A. Ranjbar, (**2015**) A parametric investigation of a PCM based pin fin heat sink, *Mech. Sci*. 6 (1) 65–73.

R. Schmidt, (**2004**) Challenges in electronic cooling—opportunities for enhanced thermal management techniques-microprocessor liquid cooled mini channel heat sink, *Heat Transfer Engineering* 25 (3) 3–12.

S. Mancin et al., (**2015**) Experimental analysis of phase change phenomenon of paraffin waxes embedded in copper foams, *Int. J. Therm. Sci*. 90 79–89.

S.K. Saha, K. Srinivasan, et al. (**2008**) Studies on optimum distribution of fins in heat sinks filled with phase change materials, *Heat Transfer engineering* 130 (3) 034505.

S.K. Saha, P. Dutta, (**2010**) Heat transfer correlations for PCM-based heat sinks with plate fins, *Application of Thermal Engineering* 30 (16) 2485–2491.

T.D. Swanson, G.C. Birur, (**2003**) NASA thermal control technologies for robotic spacecraft, *Application of Thermal Engineering* 23 (9) 1055–1065.

V. Pal, (**2014**) Modeling and thermal analysis of heat sink with scales on fins cooled by natural convection, *Int. J. Res. Eng. Technol*. 3 (6), 359–362.